Imaging Supermassive Black Hole Accretion Flows: Magnetic Fields, Jets, and Inner Shadows

Andrew Chael
(he/him)

NHFP Fellow
Princeton University

9/27/2021

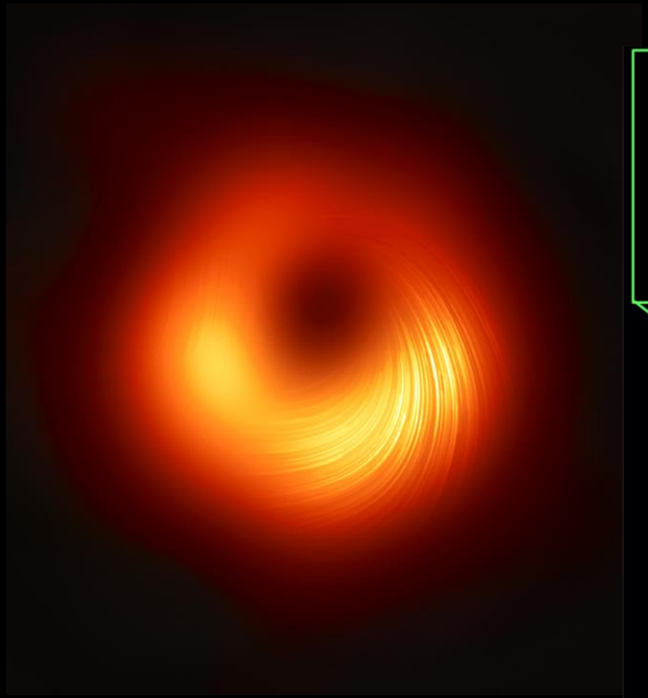

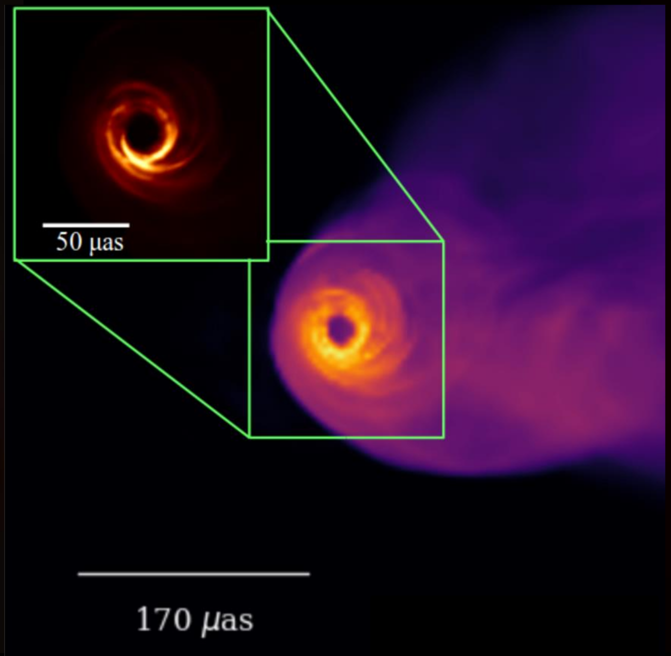

NHFP NASA Hubble Fellowship Program

PRINCETON UNIVERSITY

Event Horizon Telescope

M87

$M_{BH} = (6.5 \pm 0.7) \times 10^9 M_\odot$
$D = (16.8 \pm 0.8)\mathrm{Mpc}$

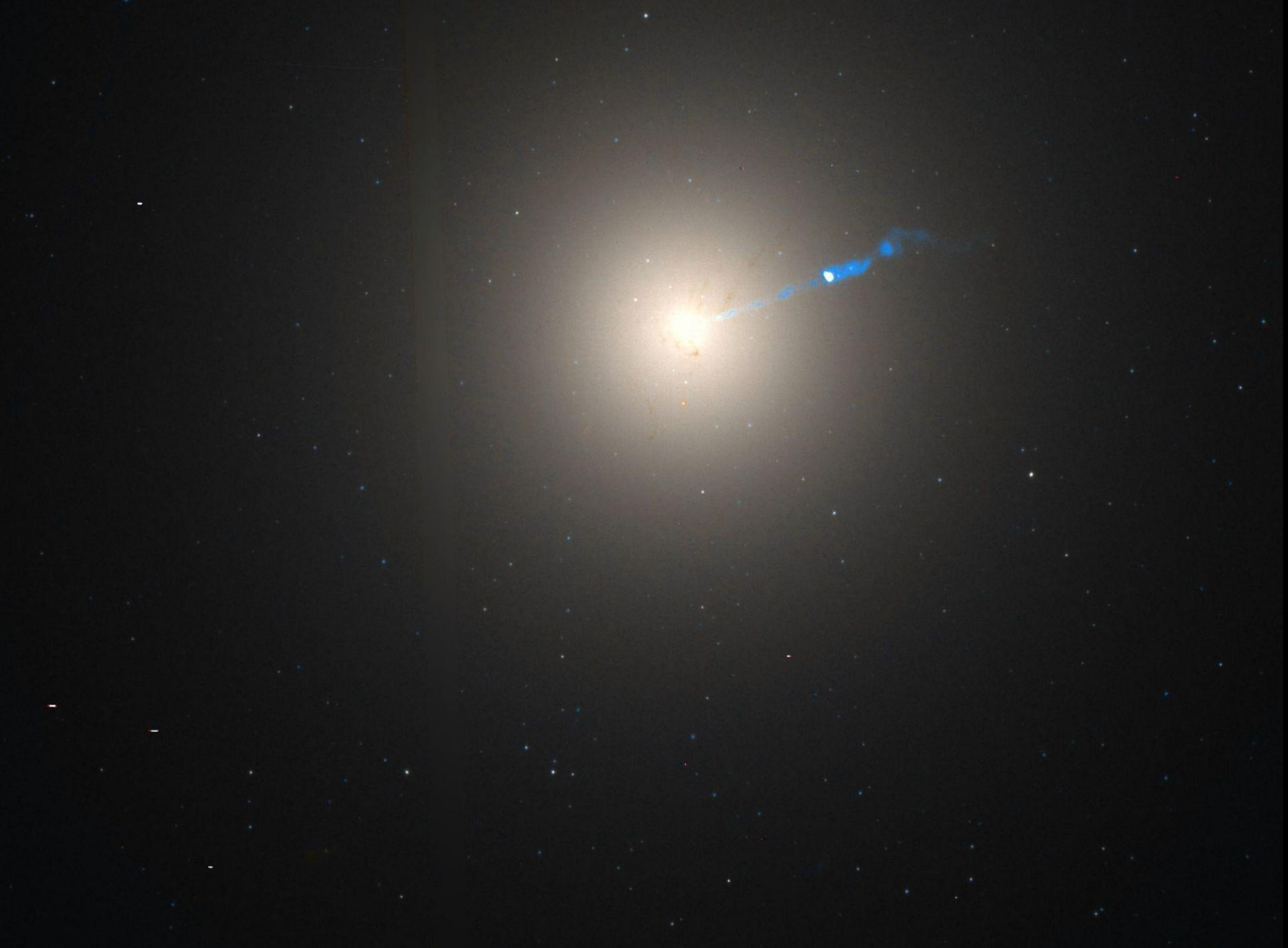

Image Credits: HST(Optical), NRAO (VLA),
Craig Walker (7mm VLBA), Kazuhiro Hada (VLBA+GBT 3mm),
EHT (1.3 mm)

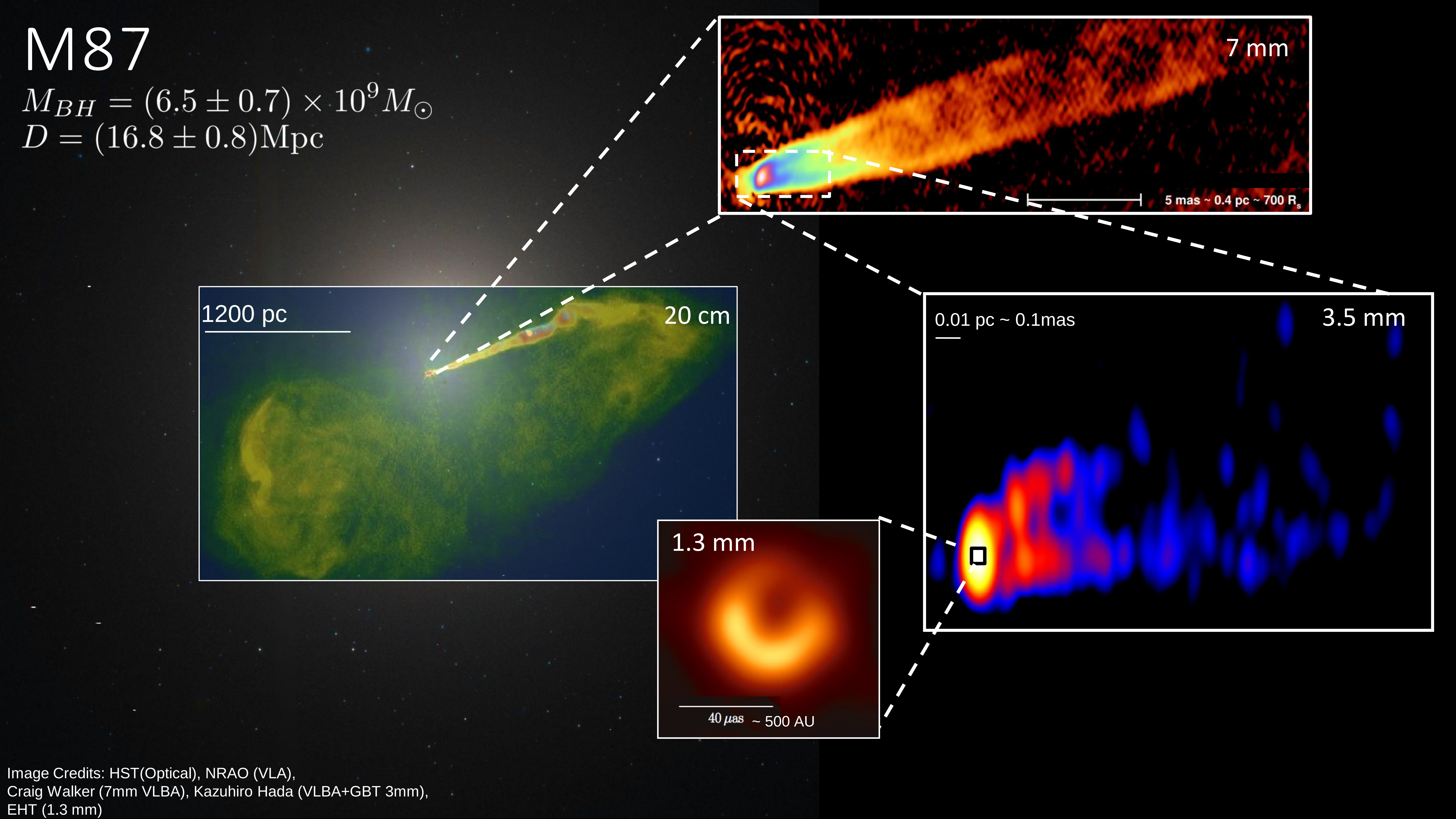
M87
$M_{BH} = (6.5 \pm 0.7) \times 10^9 M_\odot$
$D = (16.8 \pm 0.8)\mathrm{Mpc}$
7 mm
5 mas ~ 0.4 pc ~ 700 R_s
1200 pc
20 cm
0.01 pc ~ 0.1mas
3.5 mm
1.3 mm
40 μas ~ 500 AU
Image Credits: HST(Optical), NRAO (VLA),
Craig Walker (7mm VLBA), Kazuhiro Hada (VLBA+GBT 3mm),
EHT (1.3 mm)

M87* @ 230 GHz

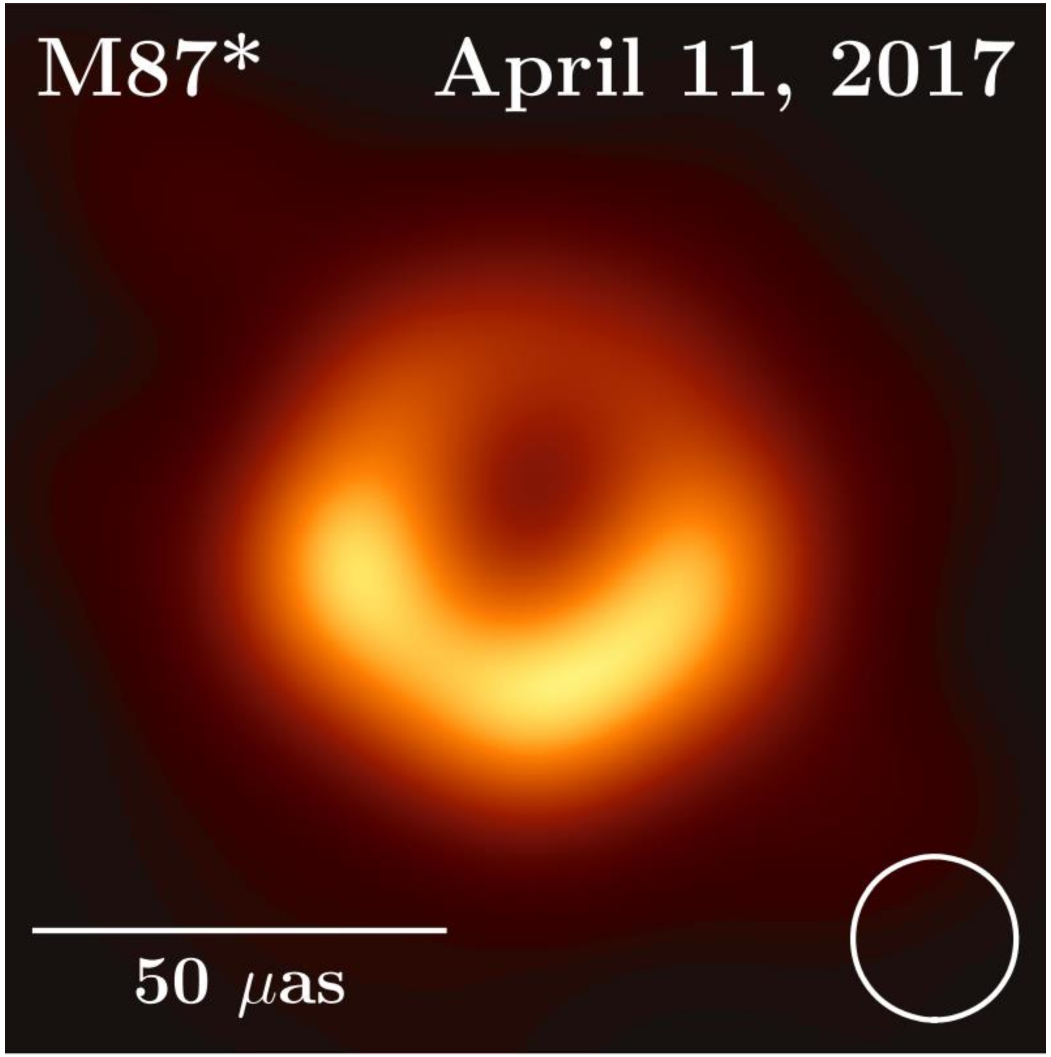

$$M = 6.5 \pm 10^9\, M_\odot$$

$$d_{\rm ring} \approx 40\,\mu{\rm as}$$
$$\approx 10^{-8}\ {\rm deg}$$
$$\approx 650\,{\rm AU}$$
$$\approx 5\,R_{\rm Sch}$$

EHTC+ 2019

The Event Horizon Telescope

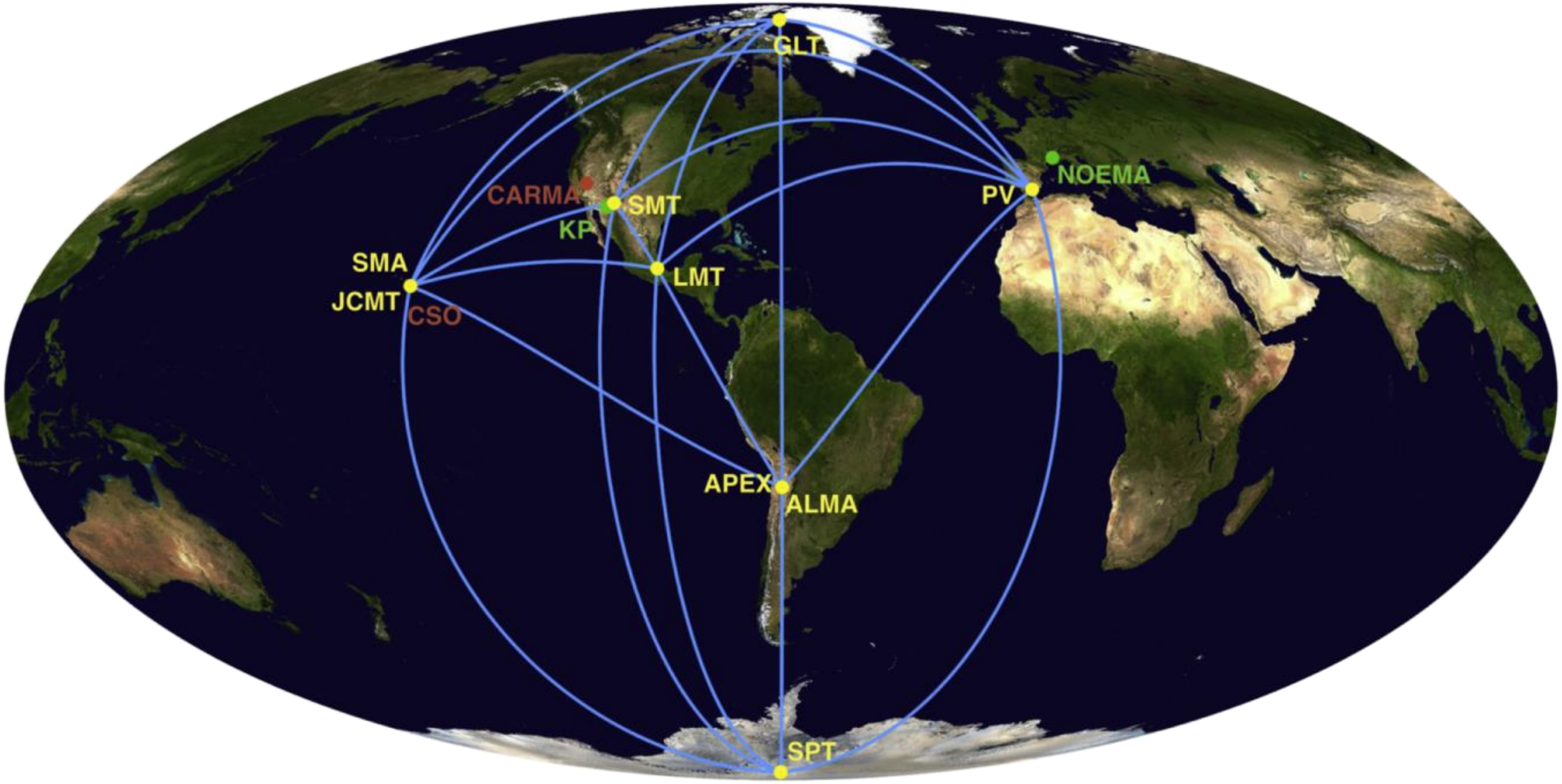

$$\text{Resolution} \approx \frac{\lambda}{d_{\text{Earth}}} \approx \frac{1.3\,\text{mm}}{1.3 \times 10^{10}\,\text{mm}} \approx 20\,\mu\text{as}$$

EHTC+ 2019 (Paper II)

At the heart of M87...

What we know:

- Supermassive black hole with mass $M \approx 6 \times 10^9 M_\odot$
- Synchrotron Emission from very hot ($T \gtrsim 10^{10}\,\mathrm{K}$) plasma close to the event horizon
- Launches a powerful relativistic jet ($P_{\rm jet} \geq 10^{42}\ \mathrm{erg\ s^{-1}}$) outside of the galaxy

Open Questions:

- Where exactly does the emission come from?
- What is the temperature and distribution of the emitting particles?
- What is the strength and configuration of the magnetic field?
- What will we see with an enhanced, next-generation EHT?

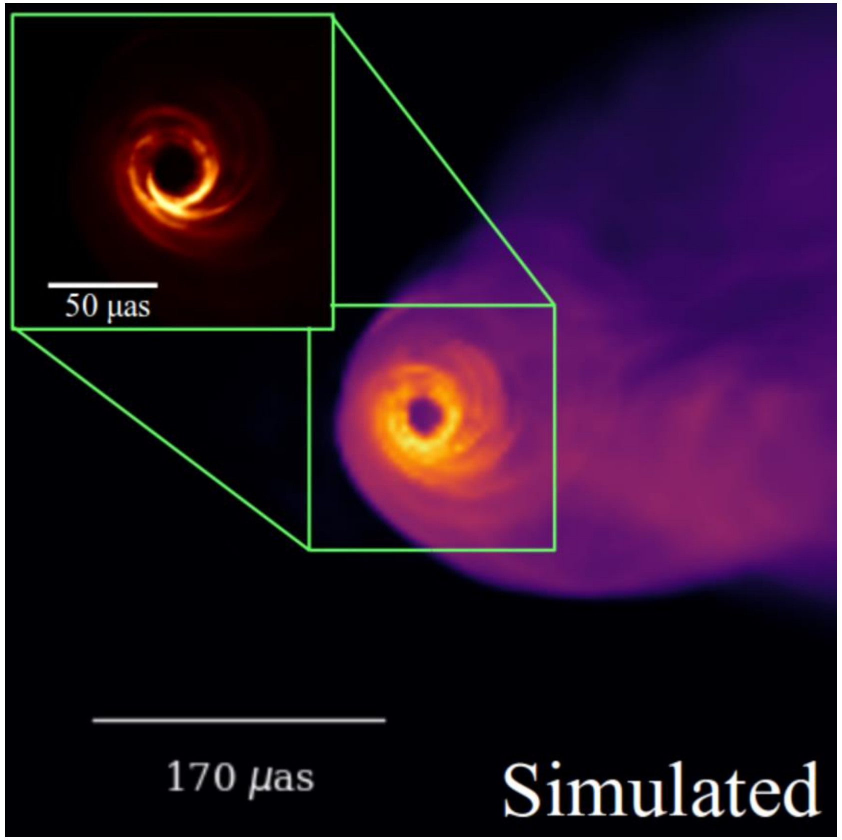

Image credit: Andrew Chael, Lindy Blackburn

Outline

1. Q: What do polarized images of M87* tell us about the magnetic fields near the supermassive black hole?

2. Q: What might we see in M87* with a next-generation EHT array?

What do polarized images of M87* tell us about the magnetic fields near the supermassive black hole?

The EHT Collaboration

EHTC Paper VII + VIII writing team

Monika Mościbrodzka

Iván Martí-Vidal

Sara Issaoun

Jongho Park

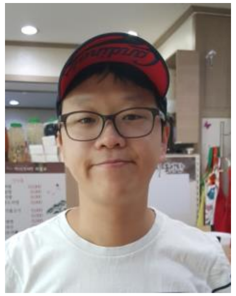

Maciek Wielgus

Angelo Ricarte

Jason Dexter

Andrew Chael

Alejandra Jiménez-Rosales

Daniel Palumbo

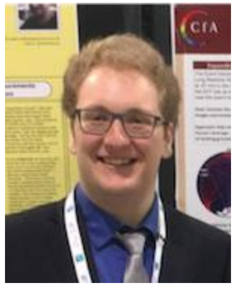

Dom Pesce

John Wardle

Avery Broderick

Ben Prather

Charles Gammie

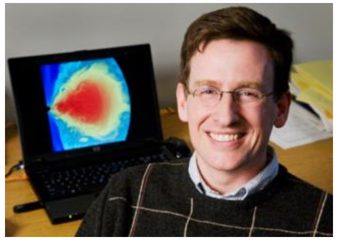

George Wong

Event Horizon Telescope

Very Long Baseline Interferometry (VLBI)

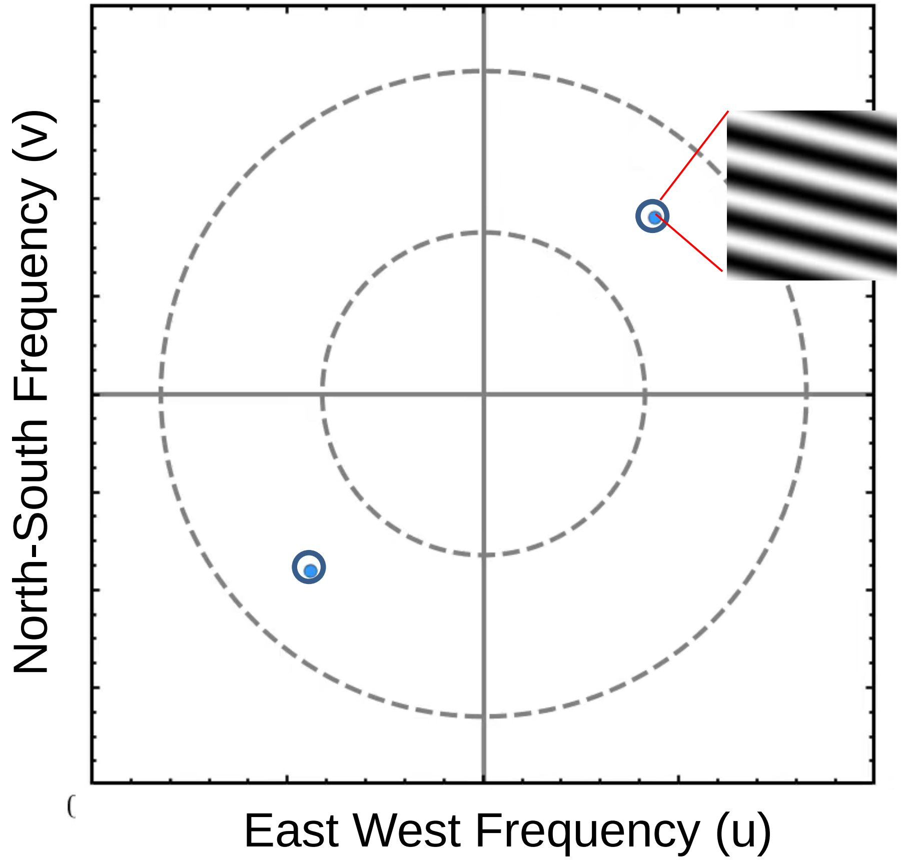

EHT coverage is **sparse**: inversion of image from the data is highly unconstrained

movie credit: Katie Bouman, Daniel Palumbo

Very Long Baseline Interferometry (VLBI)

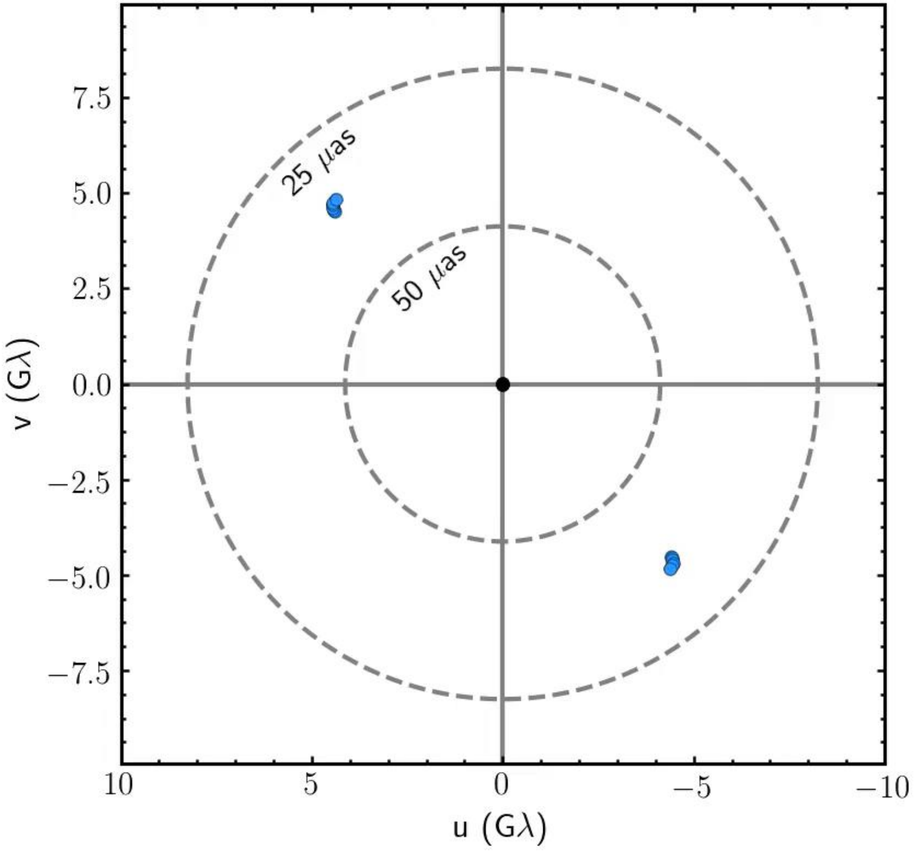

EHT coverage is **sparse**: inversion of image from the data is highly unconstrained

movie credit: Katie Bouman, Daniel Palumbo

Why polarization is hard:
Corrupting effects at EHT stations

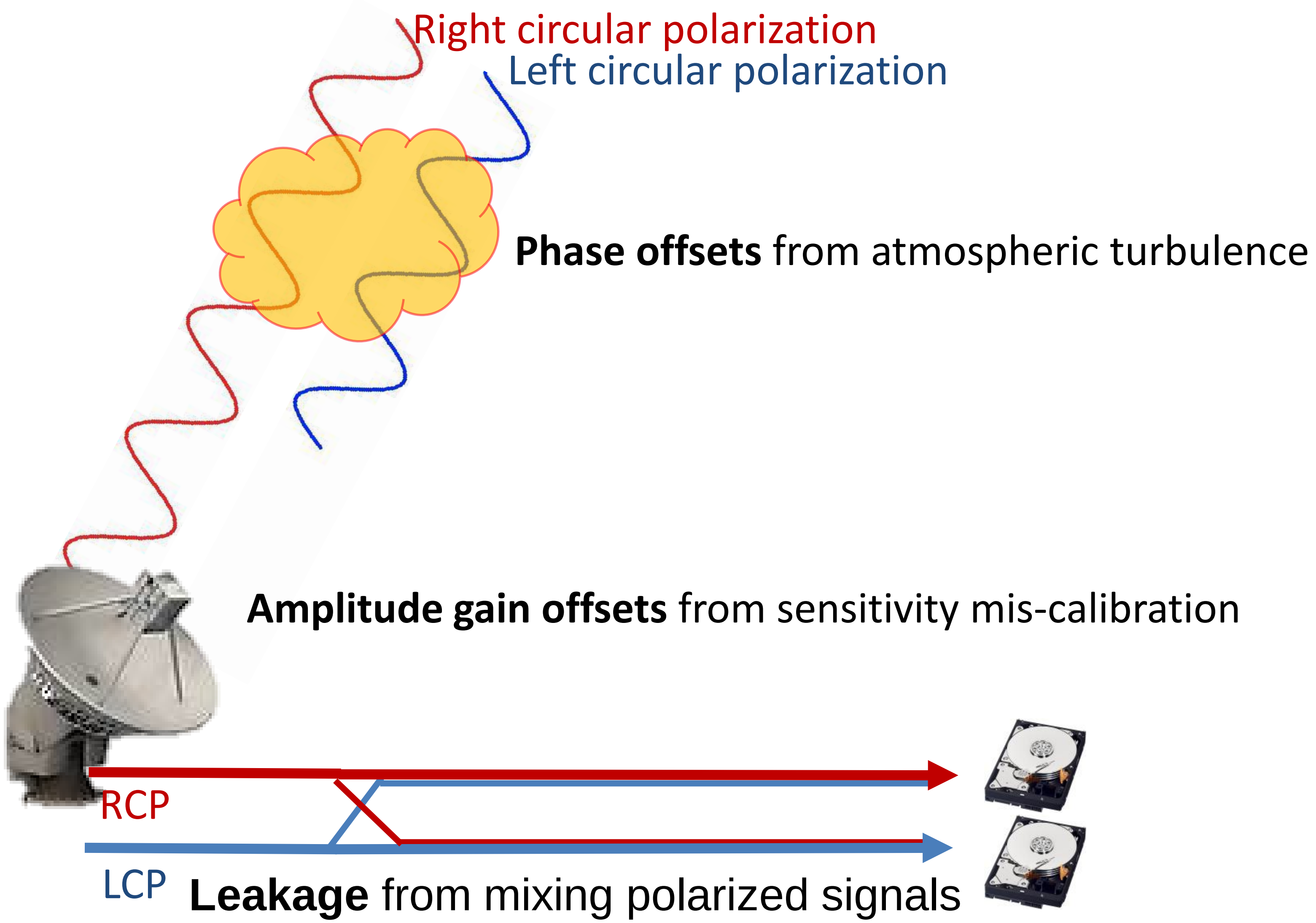

Data at each station are corrupted by unknown polarimetric **leakage** and complex gain factors

M87* in linear polarization

Total intensity

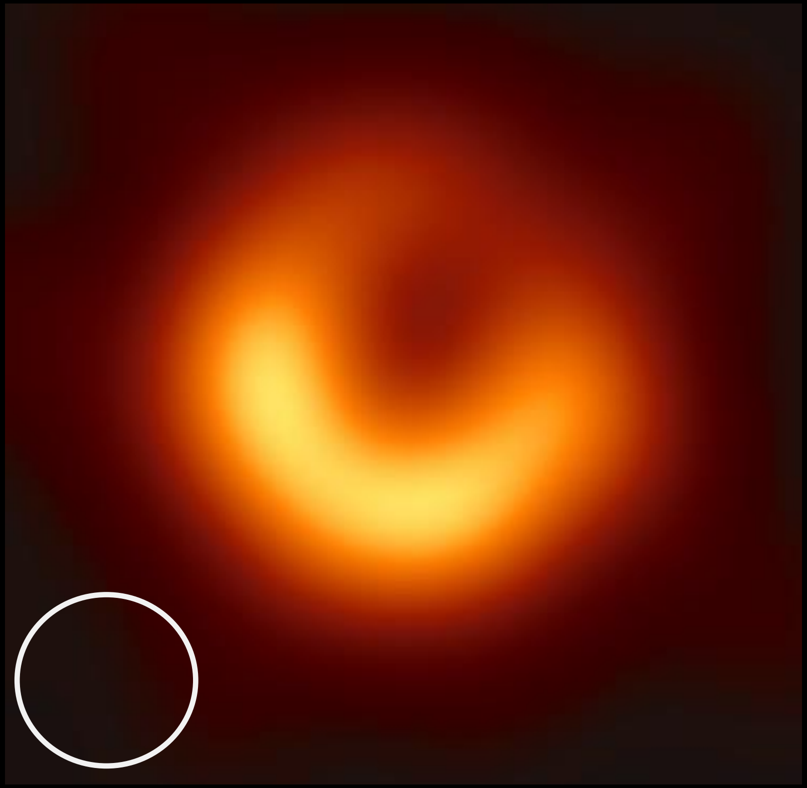

Linear Polarization

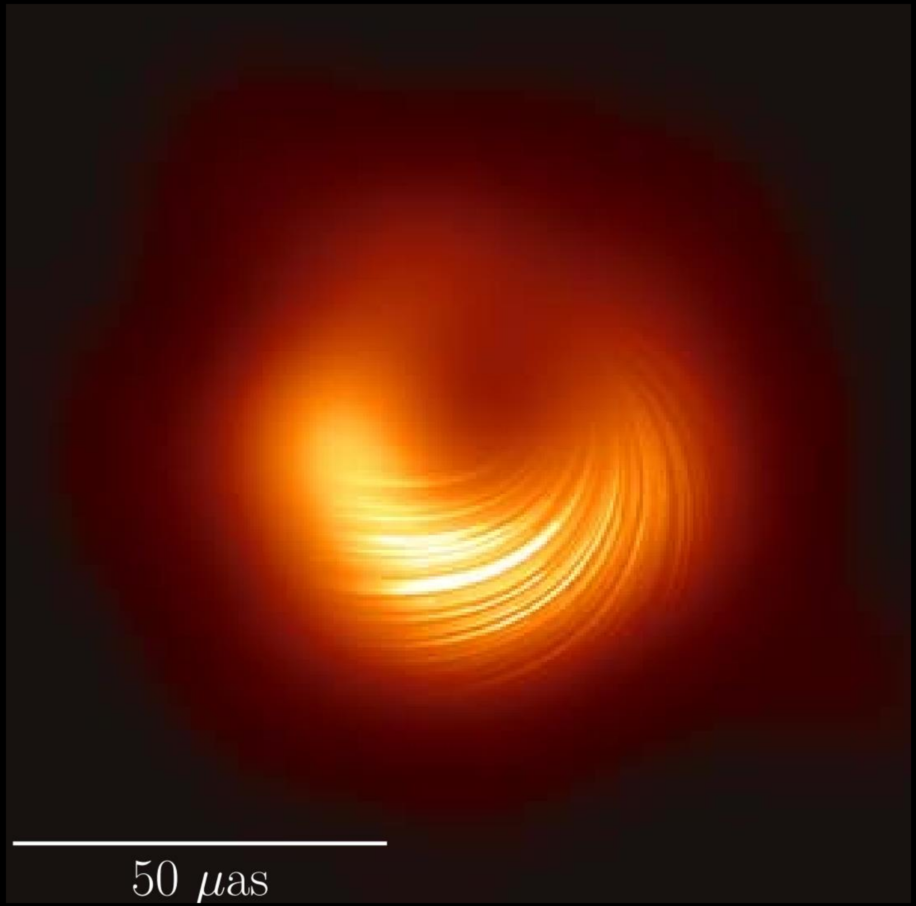

See EHTC+ 2021, Paper VII
arXiv: 2105.01169

M87* in linear polarization

Total intensity

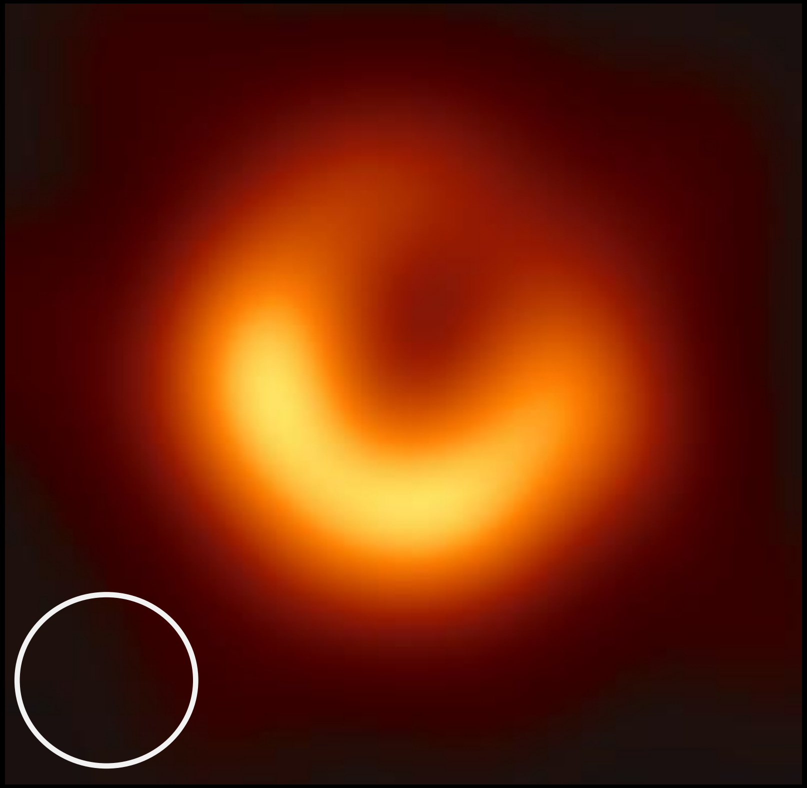

Linear Polarization

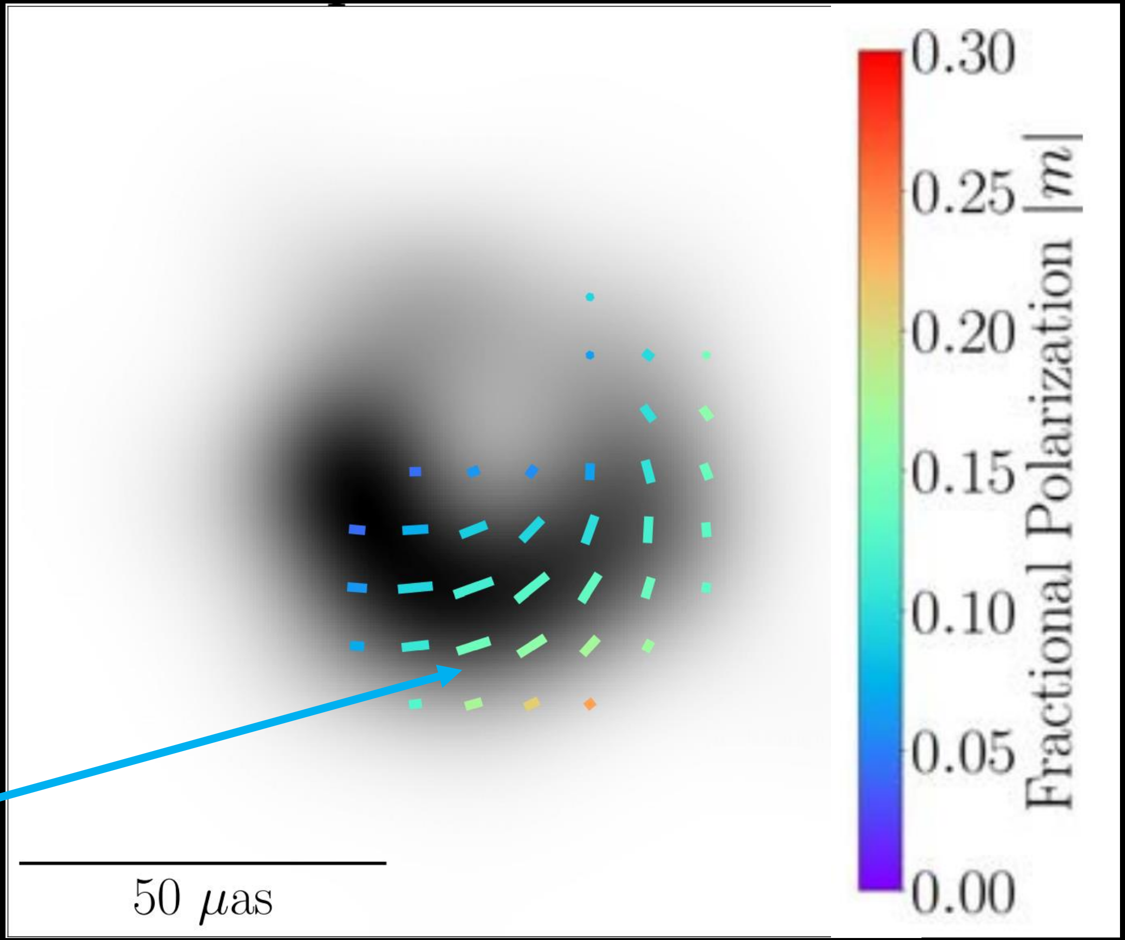

These ticks show the magnitude and direction of the linear polarization at the EHT's resolution
We can use them to learn about the magnetic fields just outside the BH event horizon

Synchrotron polarization traces magnetic fields

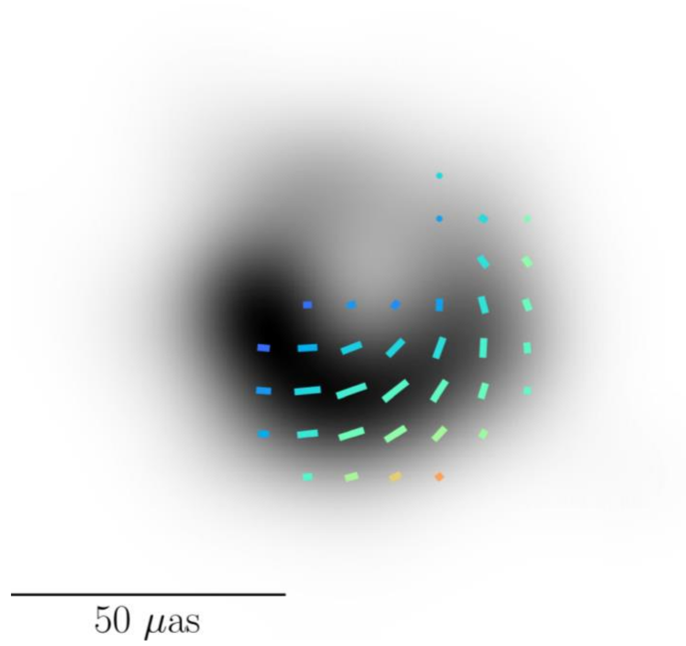

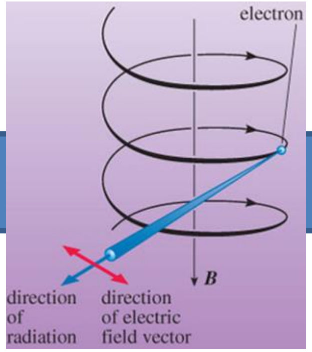

Magnetic field directions in the emission region!

Synchrotron radiation is emitted with polarization **perpendicular** to the magnetic field line

Image credit: EHTC VIII 2021, Open University

Synchrotron polarization traces magnetic fields

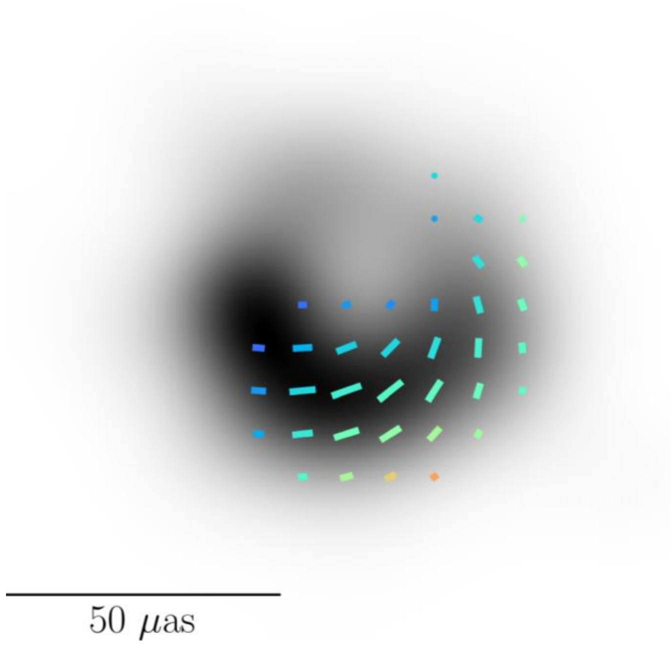

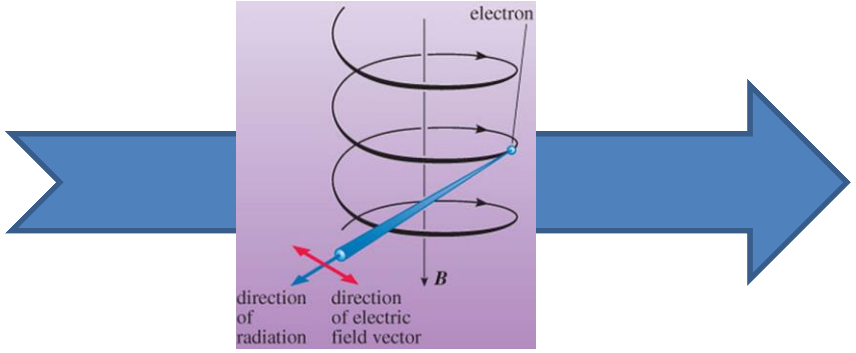

Ma tic d
dire the
emi
reg

Relativity and Faraday effects make the situation in M87* more complicated!

Image credit: EHTC VIII 2021, Open University

GR matters!

3 simple models, viewed face on

Field structure

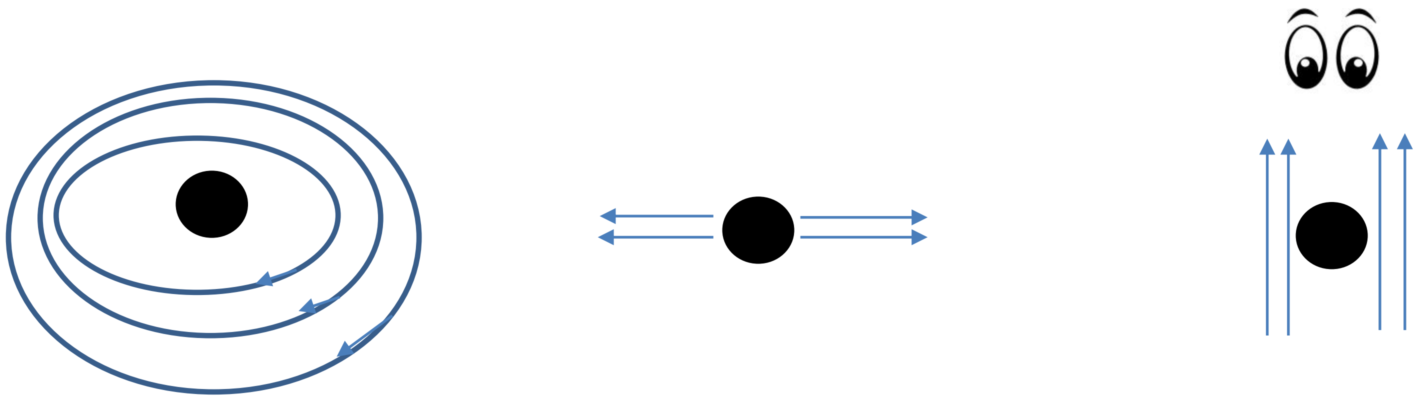

Vertical field scenario would be **unpolarized** without bent photon trajectories!

Observed image

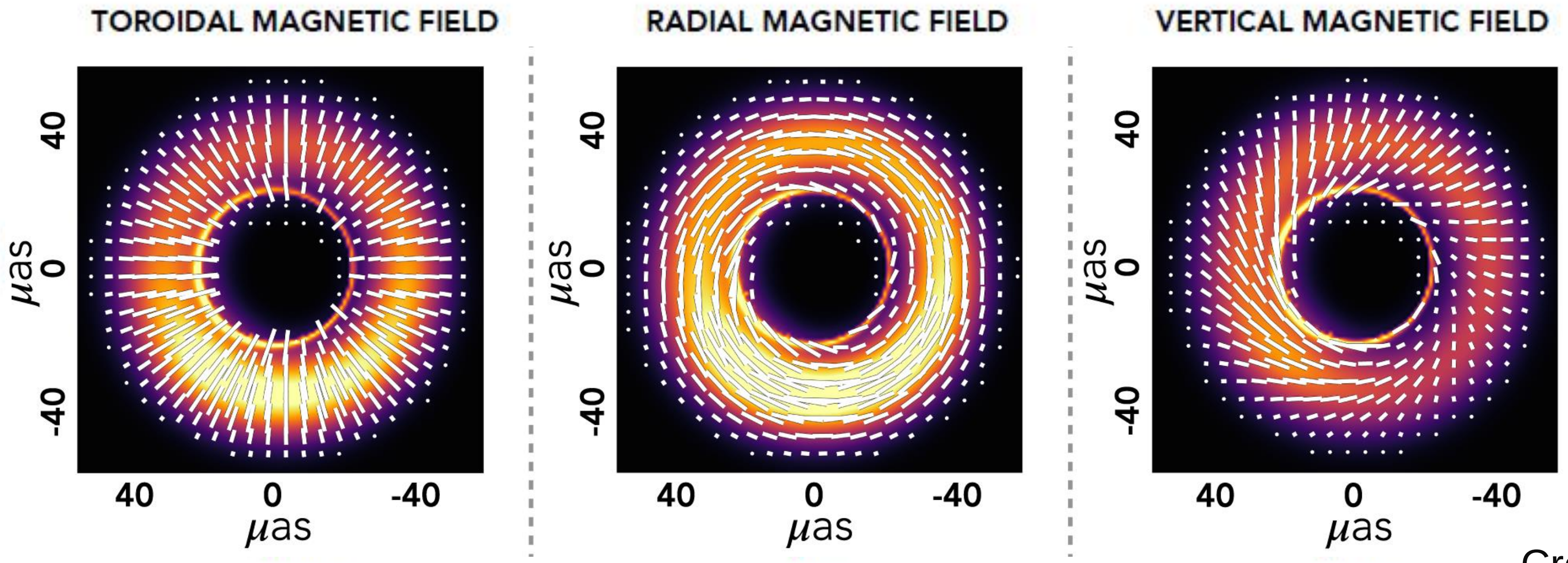

Credit: EHTC 2021 Paper VIII
Jiménez-Rosales+ 2018, Narayan+ 2021

(Internal) Faraday rotation matters!

- Significant Faraday rotation on small scales
  → **scrambles** polarization directions
  → **depolarization** of the image when blurred to EHT resolution
  → **overall rotation** of the pattern when blurred to EHT resolution

- In simulations, only significant internal Faraday rotation can produce the low fractional polarization we observe

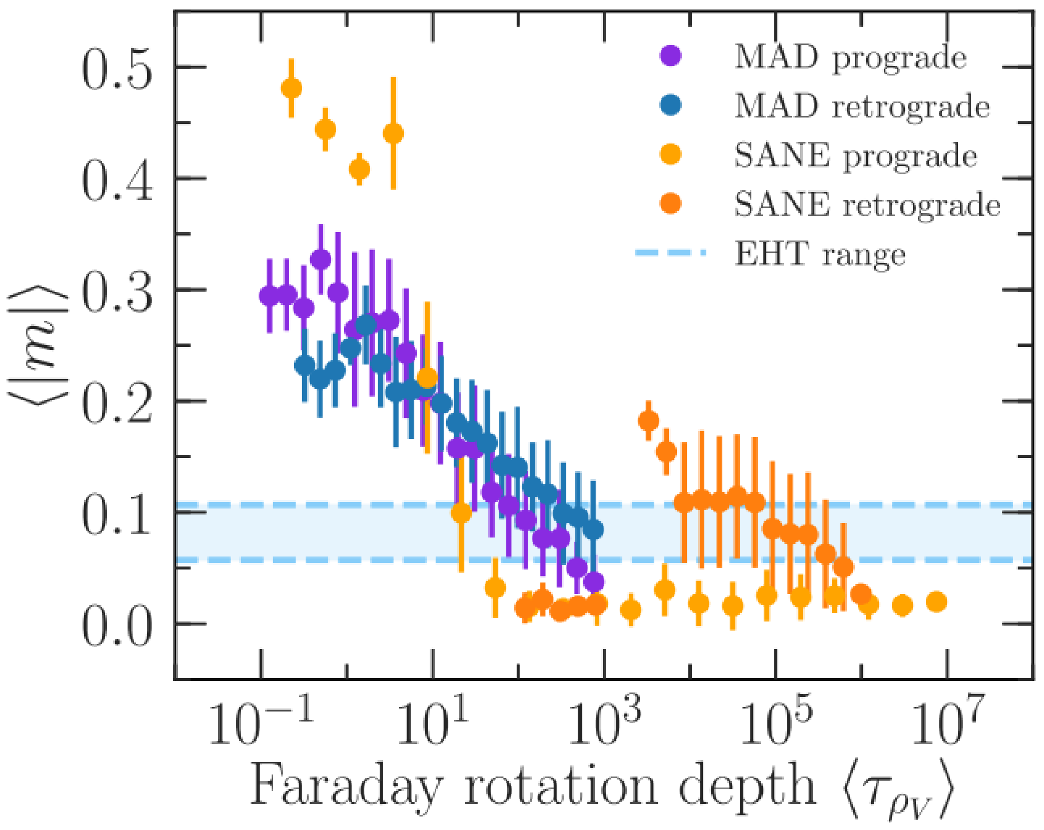

Credit: EHTC 2021 Paper VIII
Jimenez-Rosales+ 2018

Polarized images from simulations

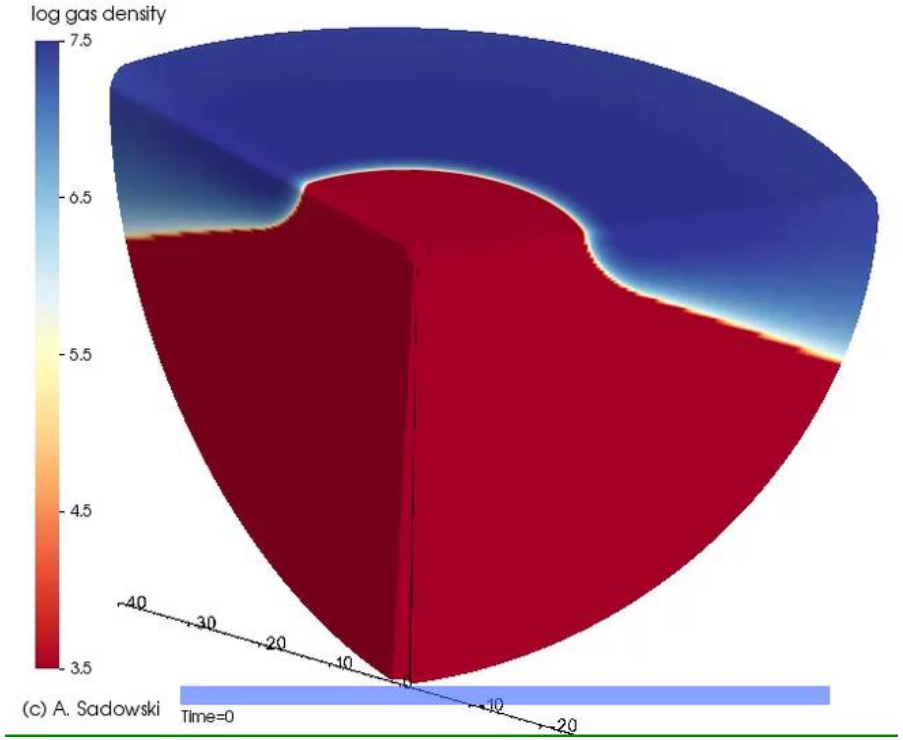

$T_e?$

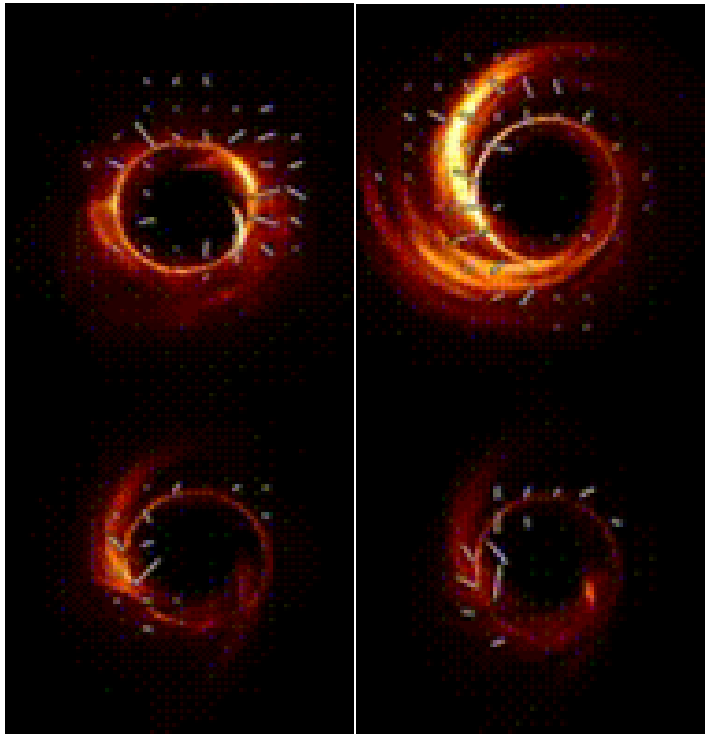

General **R**elativistic **M**agneto**H**ydro**D**ynamic (GRMHD) simulations solve coupled equations of fluid and magnetic field in Kerr spacetime

General **R**elativistic **R**adiative **T**ransfer (GRRT) codes solve for the polarized radiation (including light bending and Faraday rotation)

Movie Credits: Aleksander Sądowski (left) George Wong/Ben Prather (right)

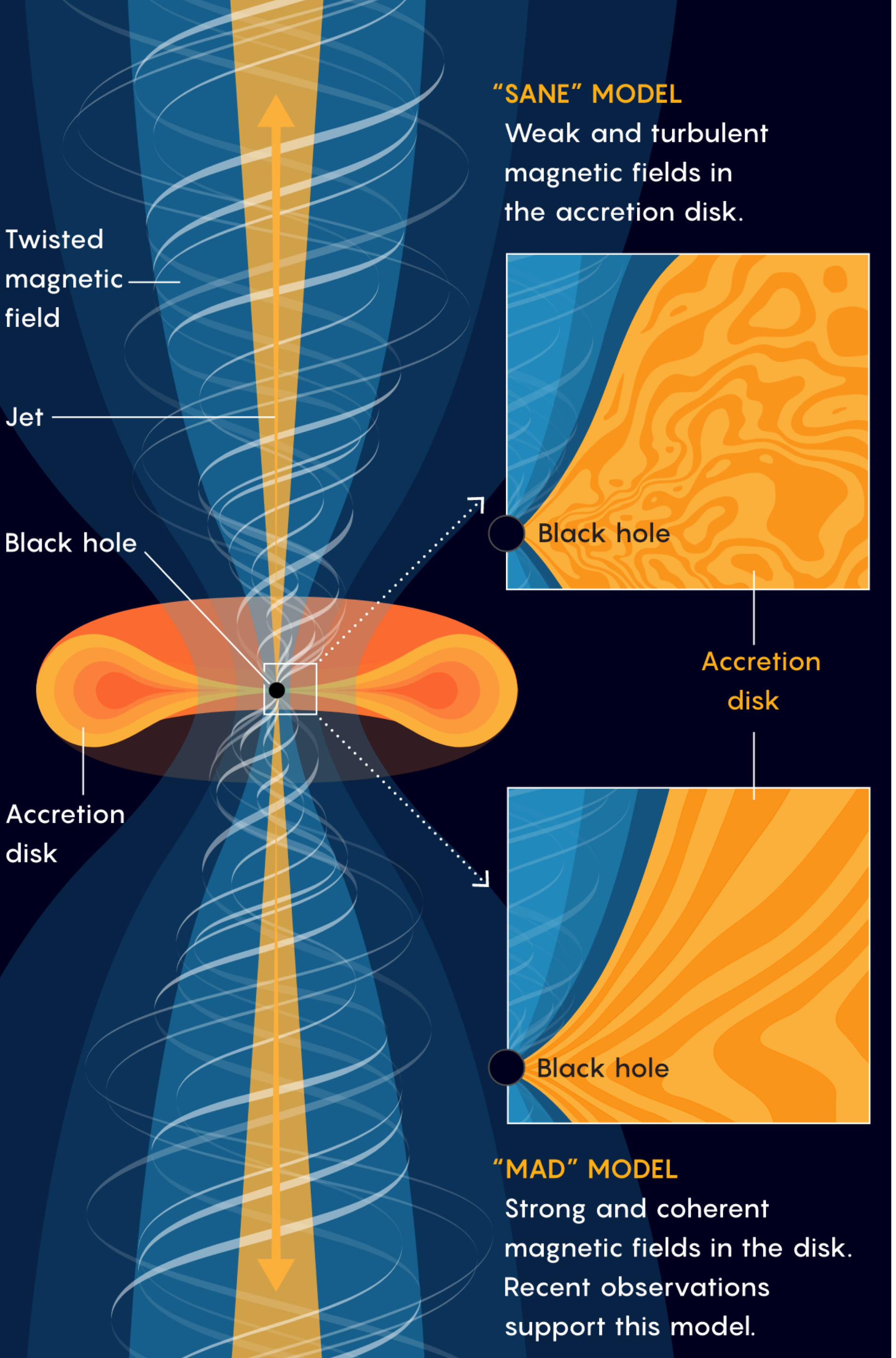

Magnetic field structure in GRMHD

Simulations show two accretion states that depend on the accumulated magnetic flux on horizon

Magnetic fields are weak and turbulent

"SANE" – Standard and "Normal" Evolution

Strong, coherent magnetic fields build up on the horizon

"MAD" - Magnetically Arrested Disk

Note: 'strong' fields mean **dynamically important ones**
→ ~10-50 G at the horizon for M87*

Igumenschchev 1977, Narayan+2003, Tchekhovskoy+2011, Narayan+ 2012
Image credit: O'Riordan+ 2017, Quanta Magazine

Simulation field structure in 3D

Fields in magnetically arrested disk (MAD) simulations have a stronger vertical component. The jet carries more power and is wider

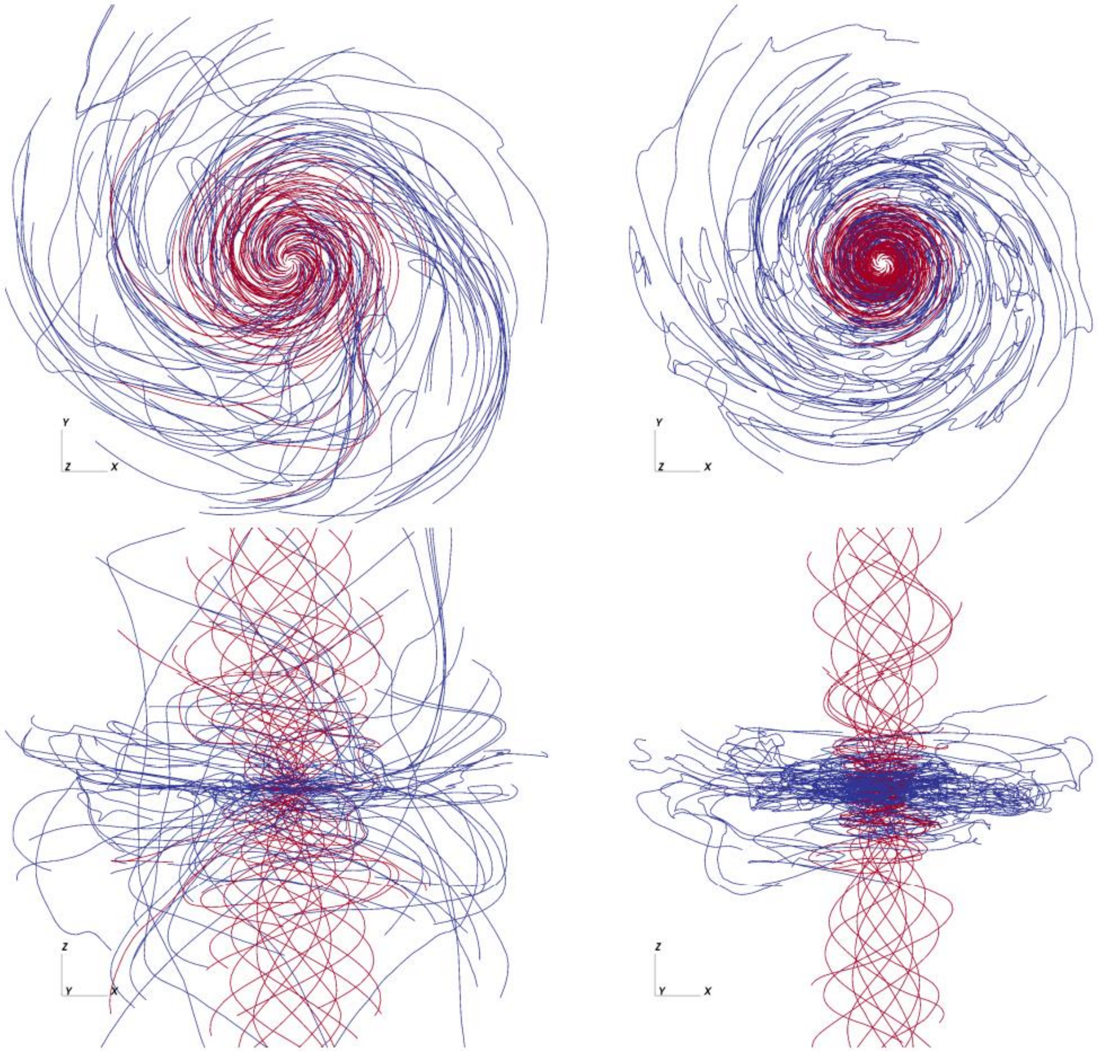

MAD

SANE

(both with spin a=0.94)

Fields in “SANE” simulations still have a helical jet, but the disk fields are relatively toroidal.

Image Credit: Angelo Ricarte
arXiv: 2104.11301

GRMHD Simulation library
2 field states, 5 spins, 72k images

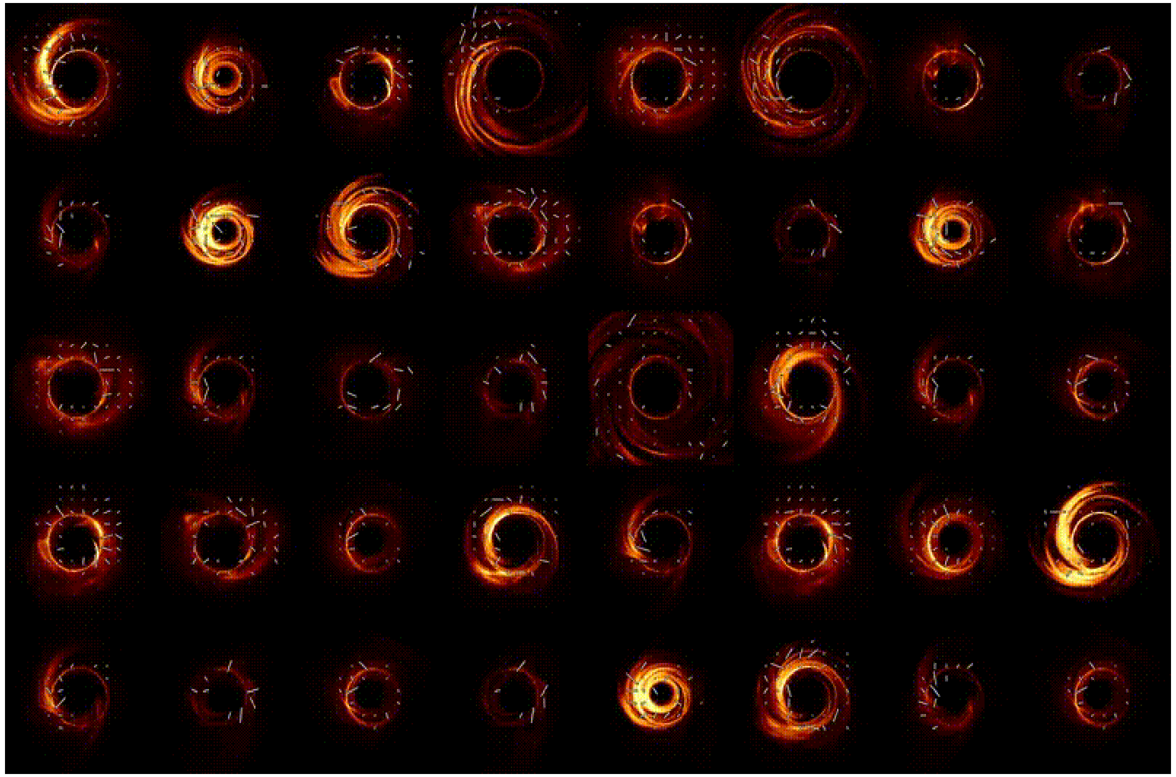

native resolution

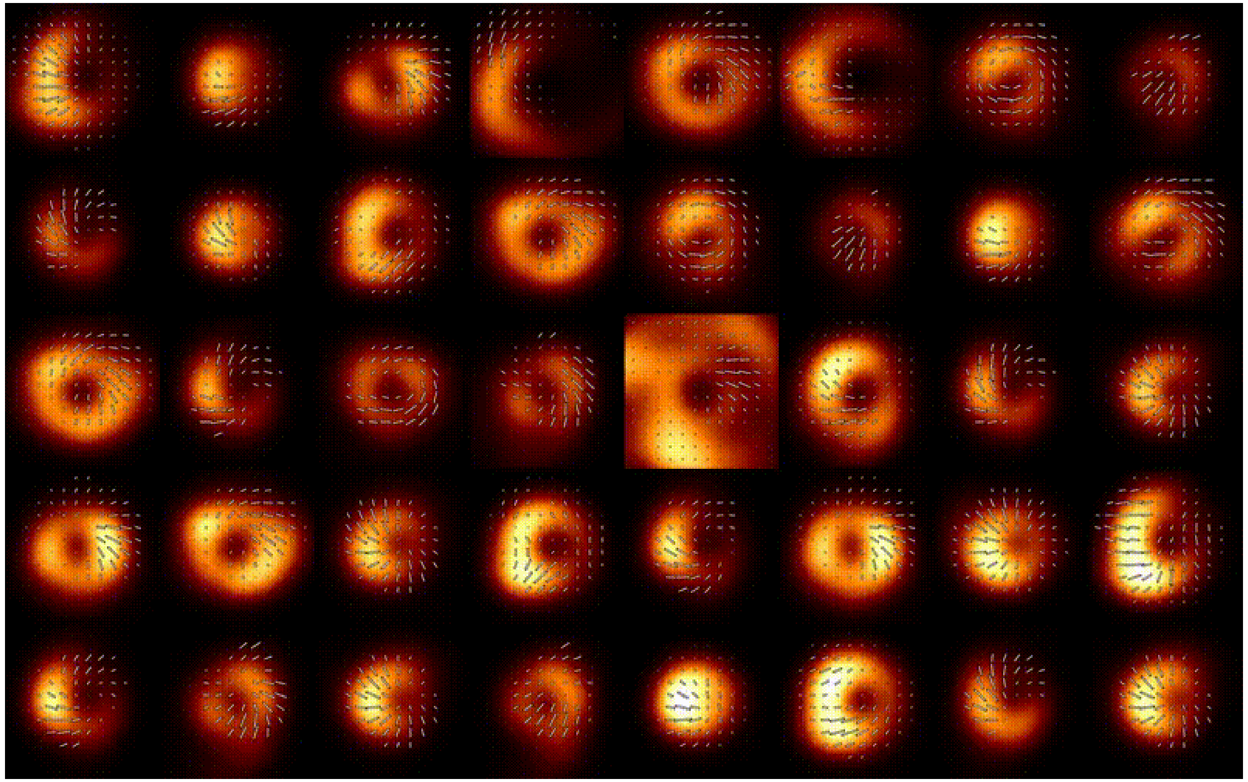

EHT resolution

Images modeled with the ipole GRRT code (Moscibrodzka & Gammie 2018)
Two-temperature plasma model from Moscibrodzka et al. 2016

$$\frac{T_i}{T_e} = R_{\rm high}\frac{\beta^2}{1+\beta^2} + R_{\rm low}\frac{1}{1+\beta^2}$$

Two parameters set the electron temperature

Animation credit: George Wong/ Ben Prather

Scoring GRMHD Simulations: before polarization
(EHTC+ 2019, Paper V)

- **Most simulation models can be made to fit total intensity observations alone** by tweaking free parameters (mass, PA, total flux density)

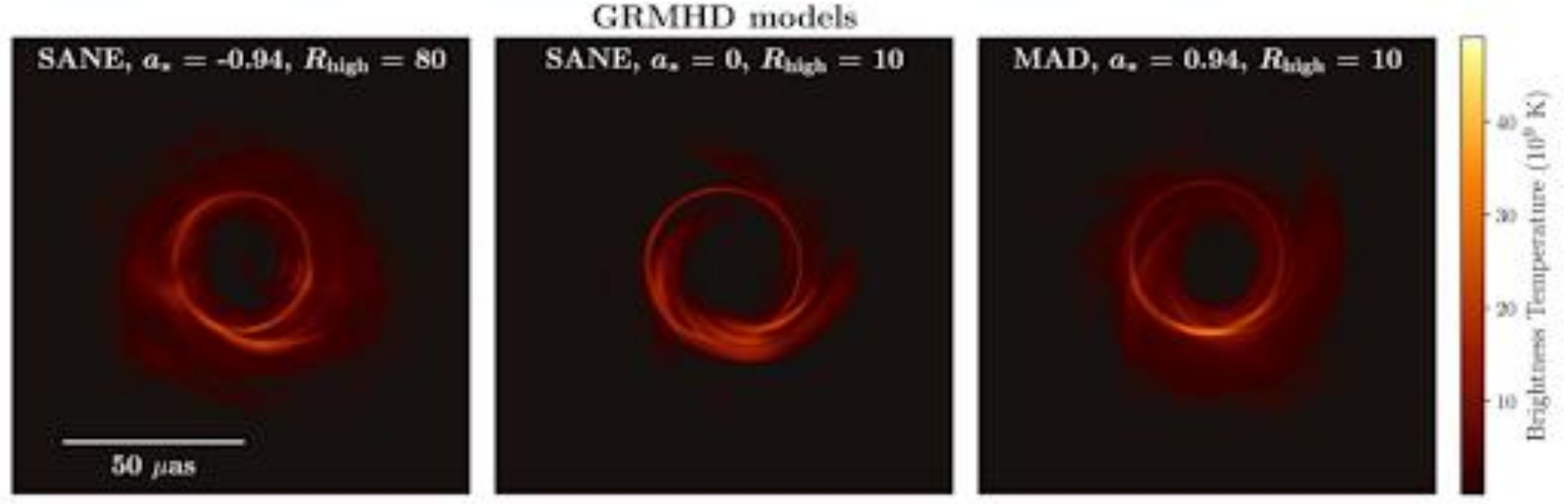

- An additional constraint on **jet power** (≥ 10^{42} erg/sec) rejects all spin 0 models
- Can we do better with polarization?

EHTC+ Paper V, 2019

Scoring simulations with polarization: Image metrics

Unresolved linear polarization fraction

$$|m|_{\rm net} = \frac{\sqrt{\left(\sum_i Q_i\right)^2 + \left(\sum_i U_i\right)^2}}{\sum_i I_i}$$

Unresolved circular polarization fraction (from ALMA)

$$|v|_{\rm net} = \frac{\left|\sum_i V_i\right|}{\sum_i I_i}$$

Average resolved polarization fraction

$$\langle |m| \rangle = \frac{\sum_i \sqrt{Q_i^2 + U_i^2}}{\sum_i I_i}$$

Azimuthal structure
2nd Fourier mode

$$\beta_2 = \frac{1}{I_{\rm ring}} \int_{\rho_{\rm min}}^{\rho_{\rm max}} \int_0^{2\pi} P(\rho,\varphi)\, e^{-2i\varphi}\; \rho\, d\varphi\, d\rho$$

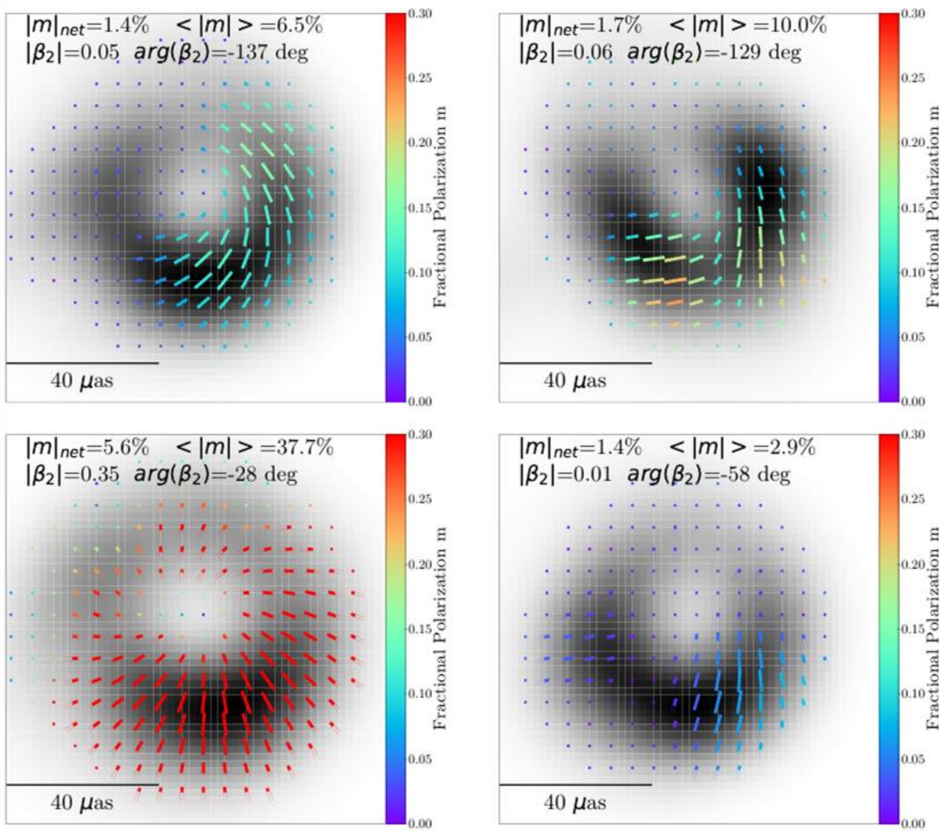

GRMHD images can be **strongly** or **weakly** polarized: with **patterns** that are radial/toroidal/helical

EHTC+ 2021 Paper VIII
arXiv: 2105.01173

Polarimetric simulation scoring

- Two scoring approaches:
  - **'simultaneous'** (demand individual images satisfy all image constraints at once)
  - Only 73 / 72,000 images satisfy all constraints simultaneously!
  - All but 2 of the passing images are from MAD simulations

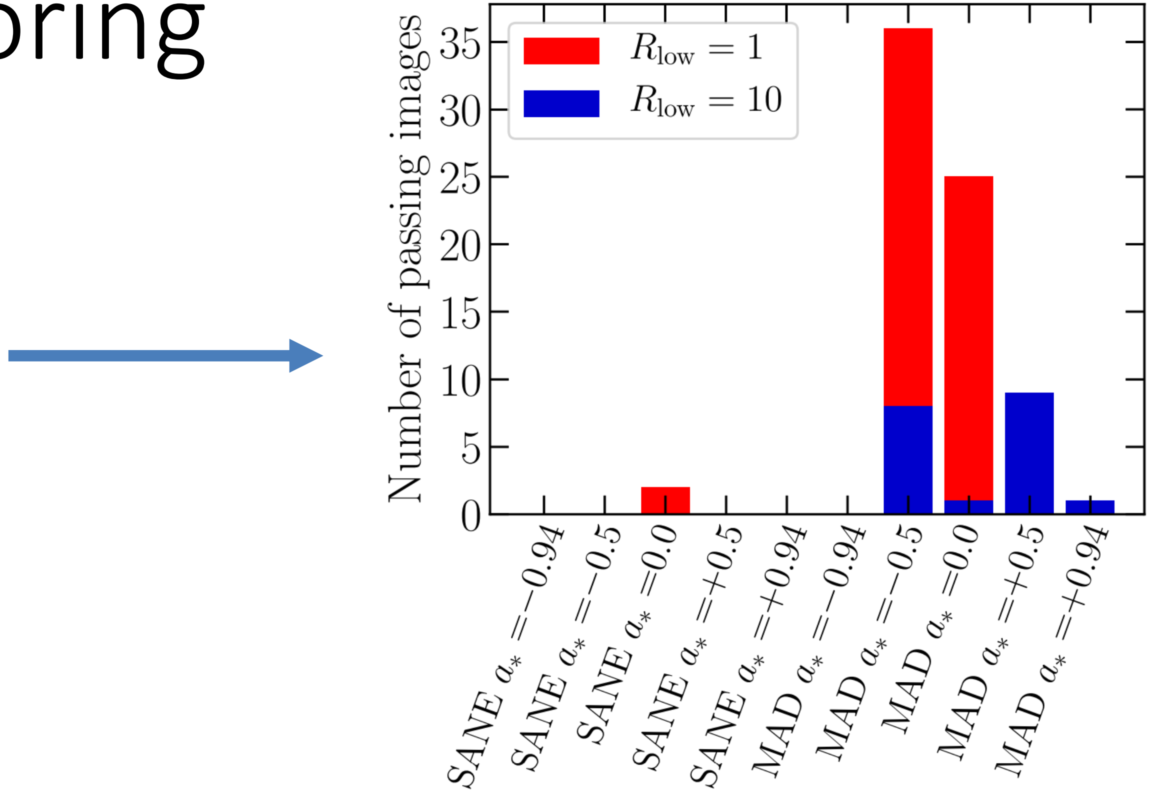

EHTC+ 2021 Paper VIII
arXiv: 2105.01173

Polarimetric simulation scoring

- Two scoring approaches:
  - **'simultaneous'** (demand individual images satisfy all image constraints at once)
  - **'joint'** (compute a likelihood comparing distance between measured quantities and simulation mean with the simulation variance)
- **Both approaches strongly favor magnetically arrested (MAD) simulations**
- The two approaches differ in which electron heating parameters they favor.
- An additional constraint on the jet power rejects all surviving non-MAD simulations (and all spin-zero simulations)

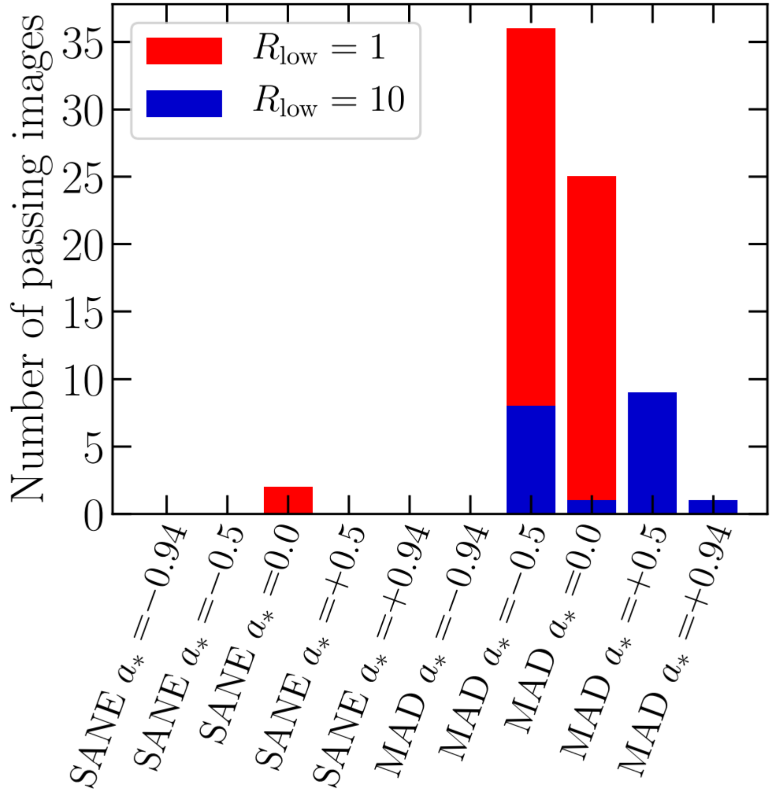

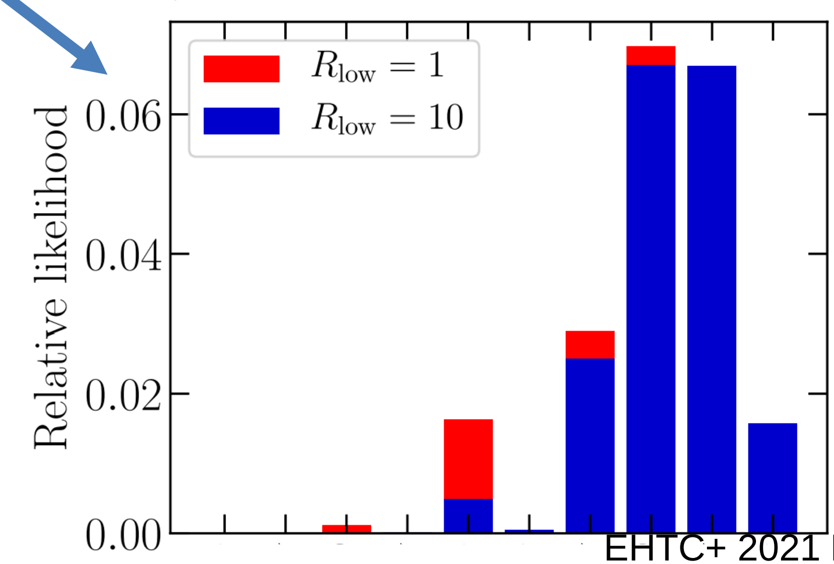

EHTC+ 2021 Paper VIII

Implications for M87*'s accretion flow

- Surviving models significantly tighten constraints on accretion rate from total intensity results:

$$\dot{M} \simeq (3-20) \times 10^{-4} M_{\odot}\,\mathrm{yr}^{-1}$$

- Constrains the electron temperature, number density, and magnetic field strength (in agreement with estimates from simple one-zone models):

$$T_e \simeq (5-40) \times 10^{10}\ \mathrm{K}$$
$$|B| \simeq (7-30)\ \mathrm{G}$$
$$n \sim 10^{4-5}\ \mathrm{cm}^{-3}$$

- Radiative efficiency ~1%

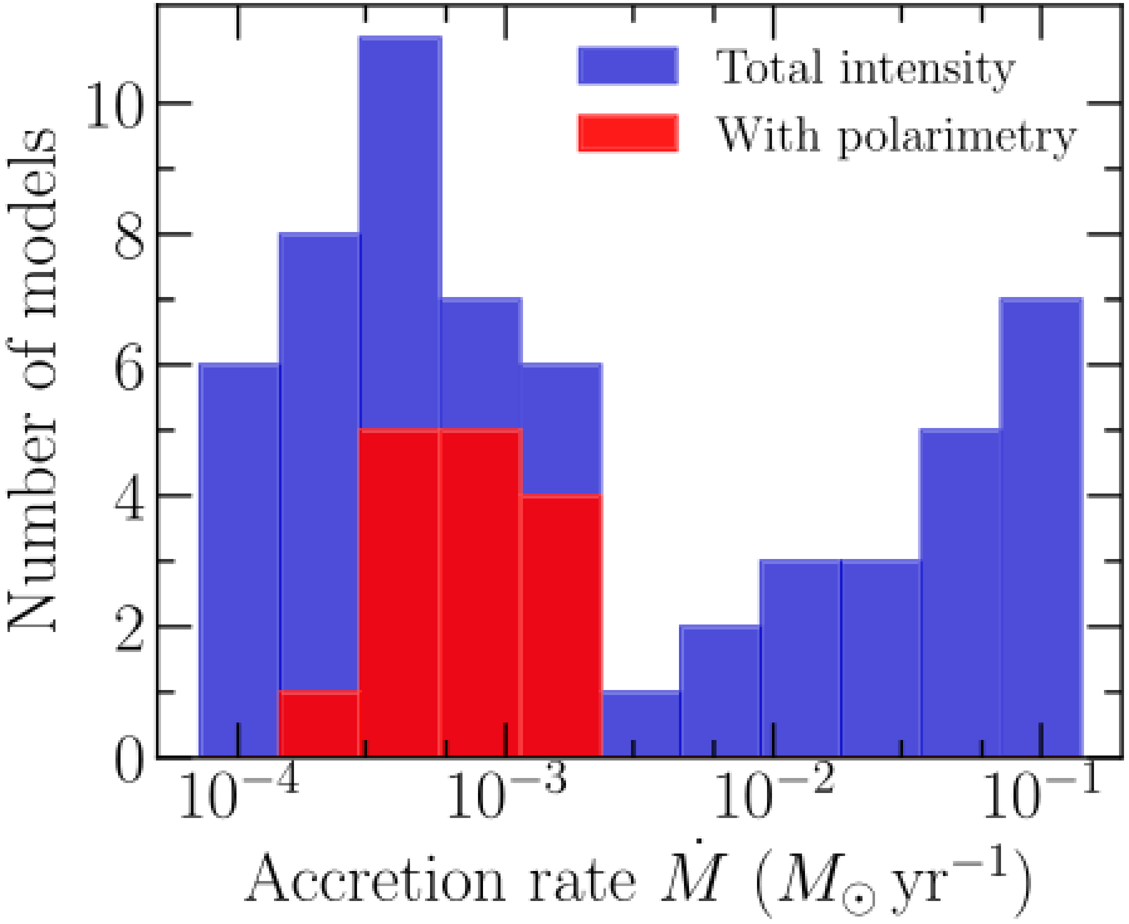

EHTC+ 2021 Paper VIII
arXiv: 2105.01173

What do polarized images of M87* tell us about the magnetic fields near the supermassive black hole?

A: Magnetic fields in M87* are strong and dynamically important: the accretion flow is **magnetically arrested**

What might we see in M87* with future observations or a next-generation EHT array?

EHT observations in the last 5 years

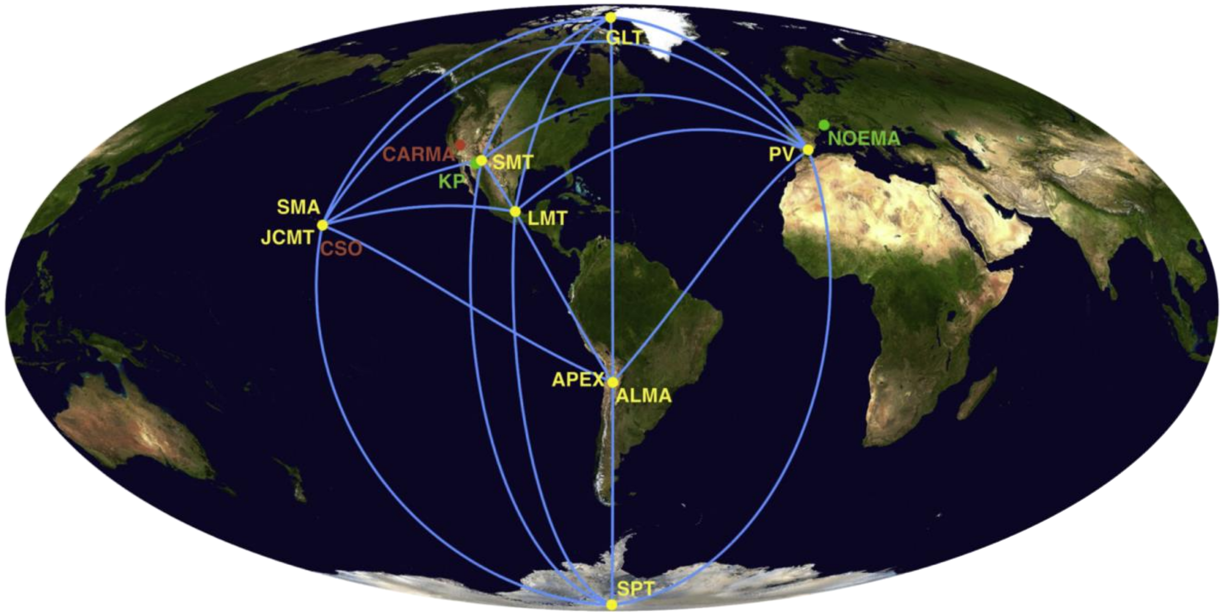

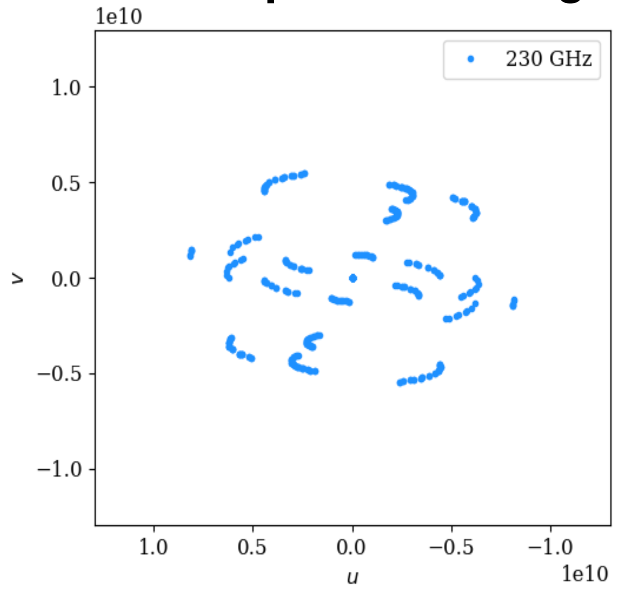

2017: Observations at 6 distinct sites
2018: Observations at 7 sites (+ GLT)
2019-2020: no observations
2021: Observations at 9 sites (+ Kitt Peak & NOEMA)

$$N_{\mathrm{obs}} = \binom{N_{\mathrm{sites}}}{2} \propto N_{\mathrm{sites}}^2$$

A next-generation EHT (ngEHT)

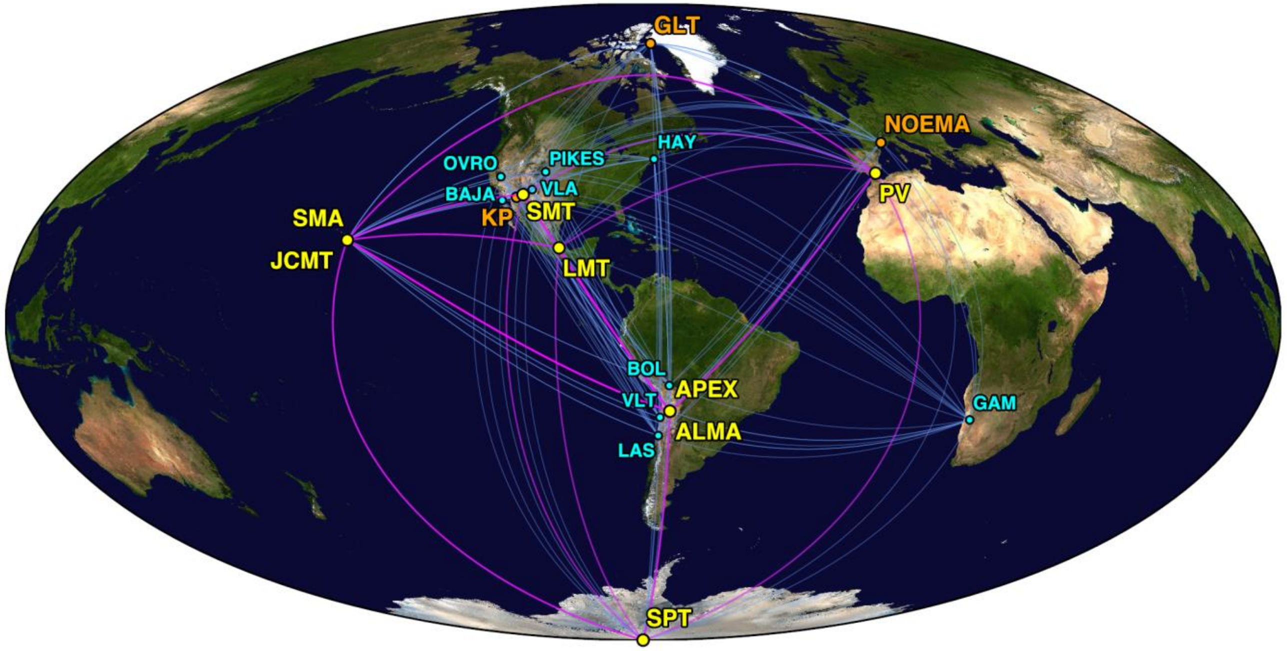

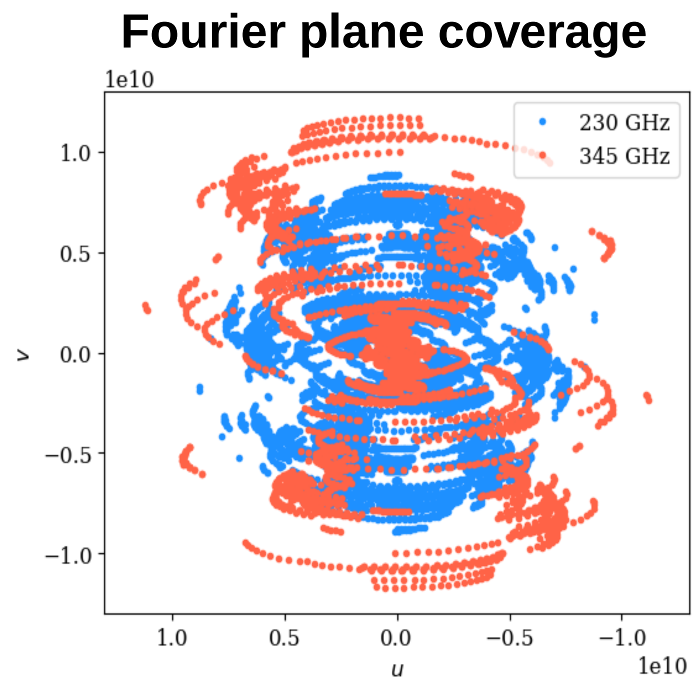

Adding 345 GHz will increase **resolution**

Increased (u,v) filling from new sites in ngEHT will enhance **dynamic range**

See the EHT Ground Astro2020 APC White Paper
(Blackburn, Doeleman+; arXiv:1909.01411)

What happens when we look at GRMHD simulation images at high dynamic range?

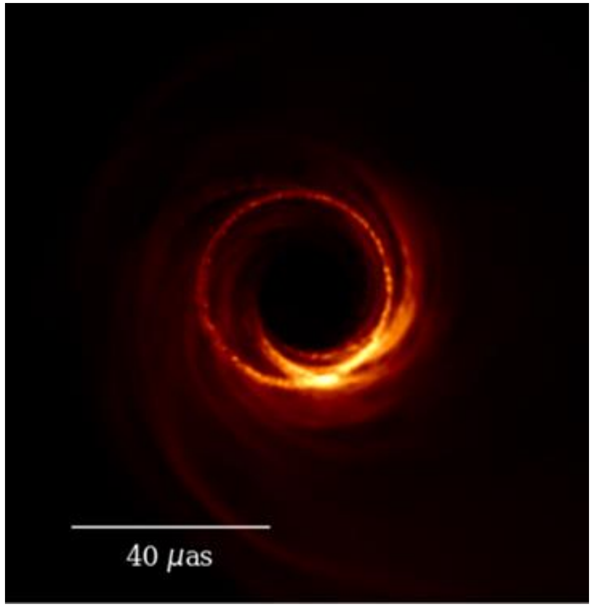

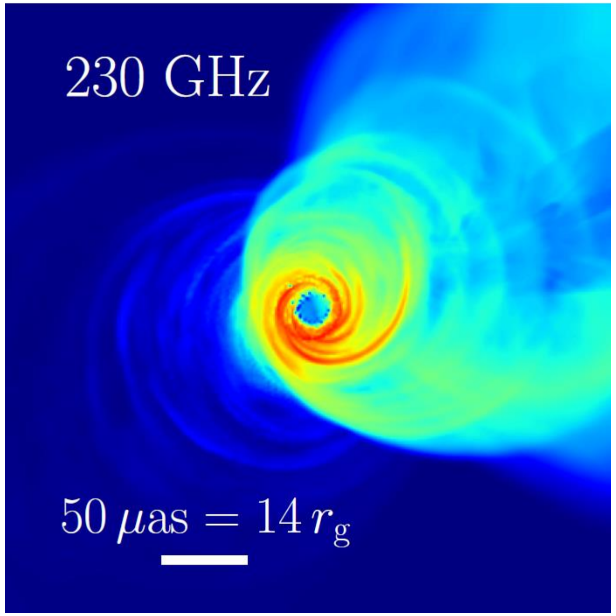

- If the simulation is run long enough and raytraced with certain electron heating prescriptions, we see a visible jet like in M87
- Future EHT observations should be able to see this dim extended jet emission around the black hole image

Radiative Simulations of magnetically arrested disks (MADs)
From Chael+ 2019 using KORAL code (Sadowski+ 2013,16)

ngEHT will illuminate the BH-jet connection

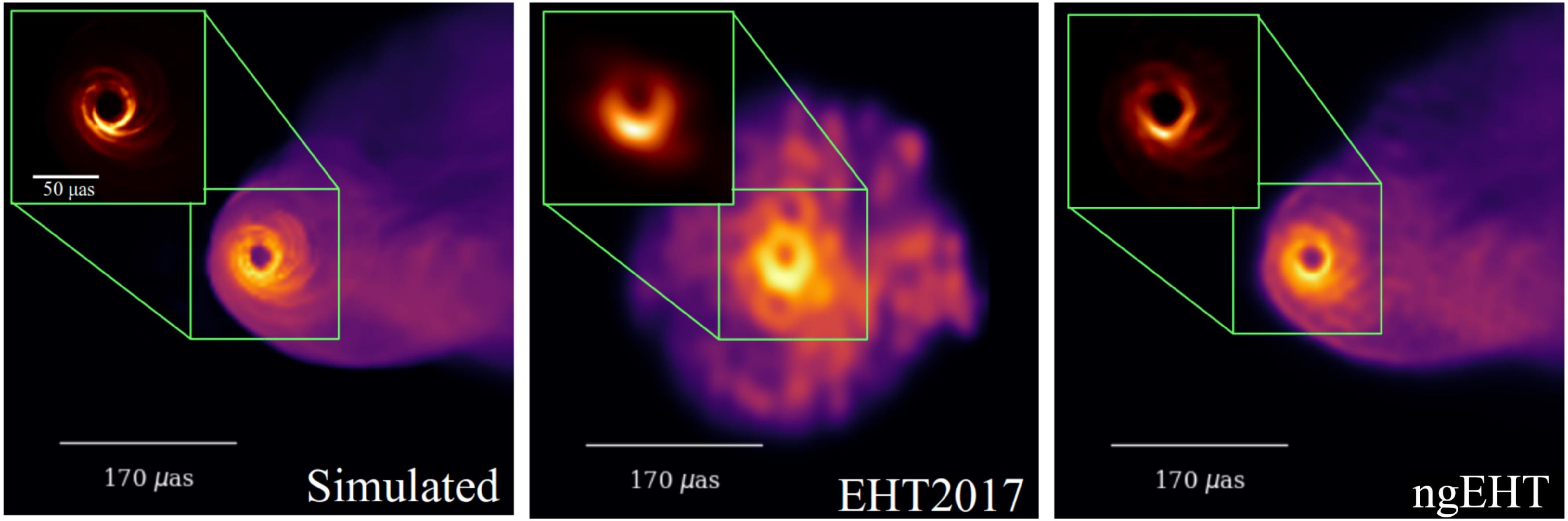

Increased u,v filling from new sites in ngEHT will enhance **dynamic range**

Going to 345 GHz will increase **resolution**

See EHT Ground Astro2020 APC White Paper
(Blackburn, Doeleman+; arXiv:1909.01411)
Simulation credit: Chael+ 2019

Jet Power & Width in long-duration MAD Simulations

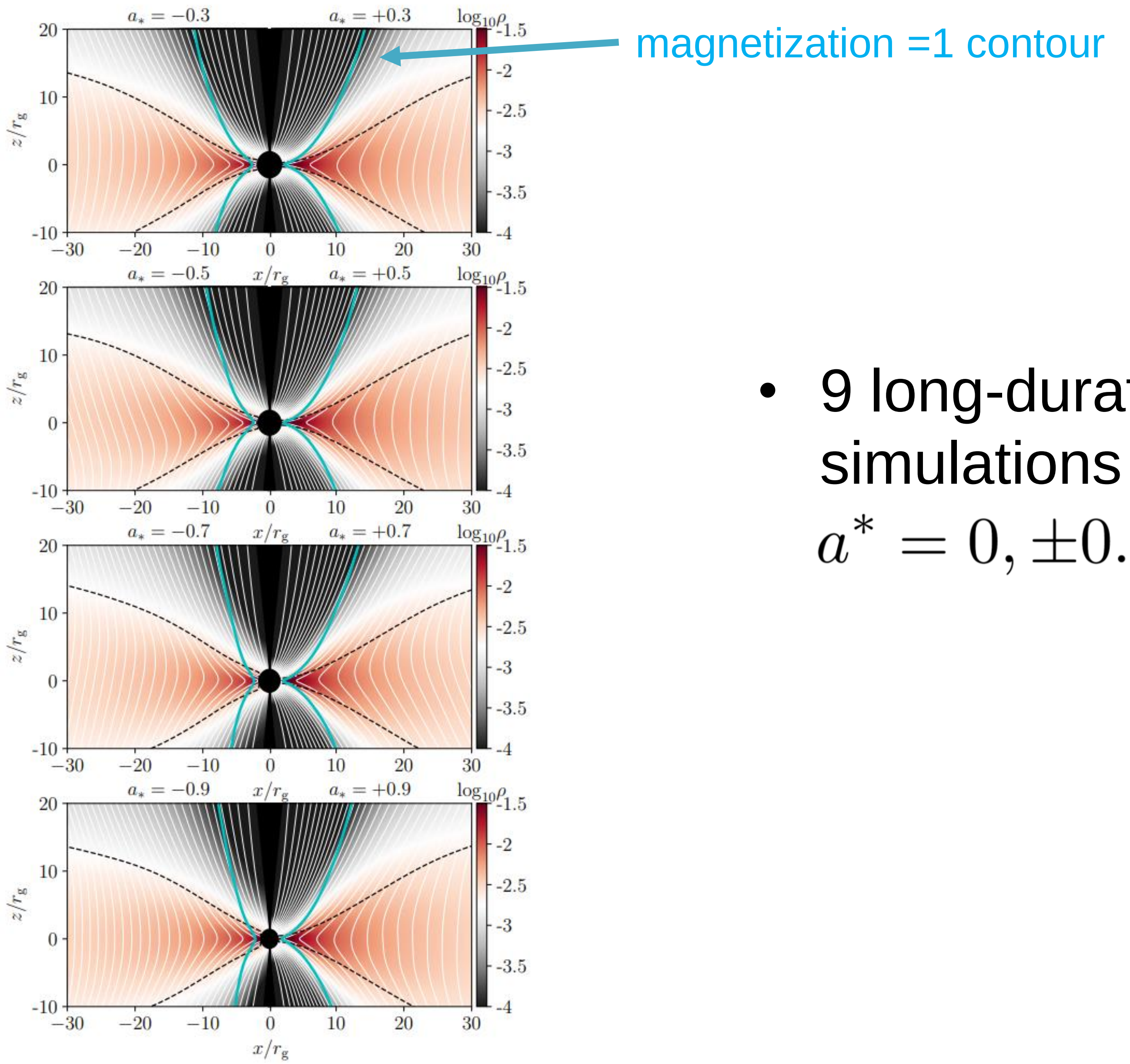

- 9 long-duration ($t_{\max} = 10^5\ GM/c^3$) MAD simulations at different black hole spins $a^* = 0, \pm 0.3, \pm 0.5, \pm 0.7, \pm 0.9$

Time-and azimuth-averaged simulation data

R. Narayan, A. Chael, K. Chatterjee, A. Ricarte, B. Curd
arXiv: 2108.12380

Jet Power & Width in long-duration MAD Simulations

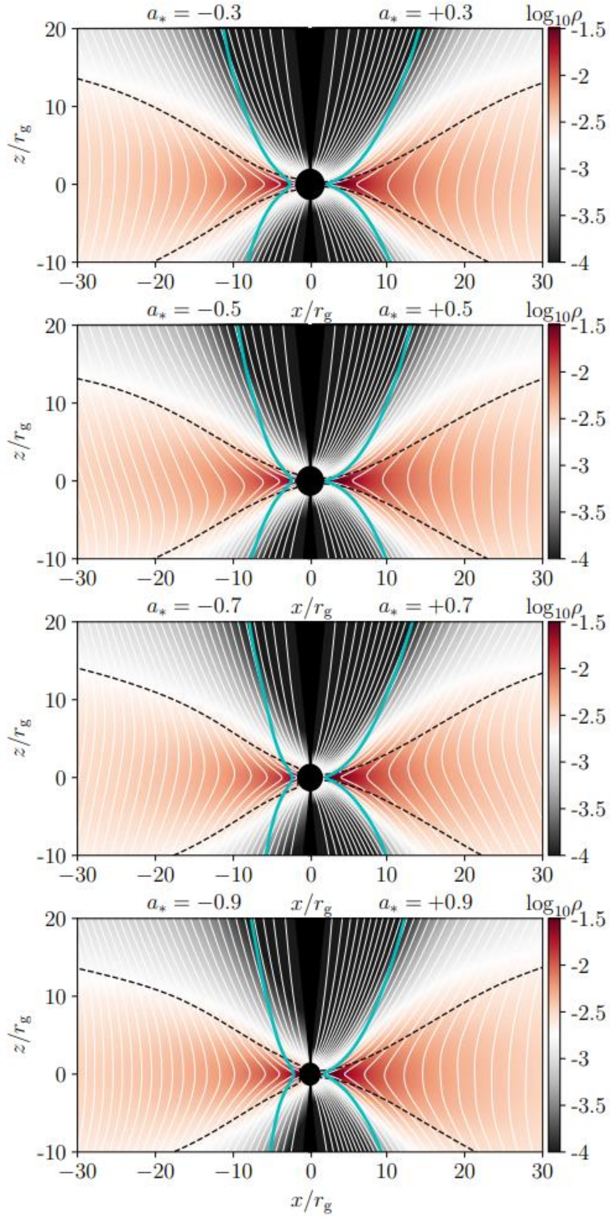

Time-and azimuth-averaged simulation data

- Jet width at the base **increases** with BH magnetic flux
- Disk height near the BH **decreases** with flux
- Both could potentially be observable with future EHT/ngEHT observations!

Disk height

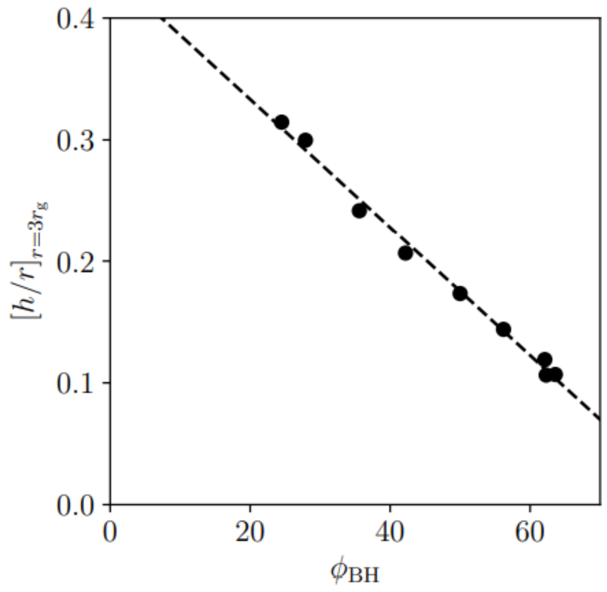

Jet width

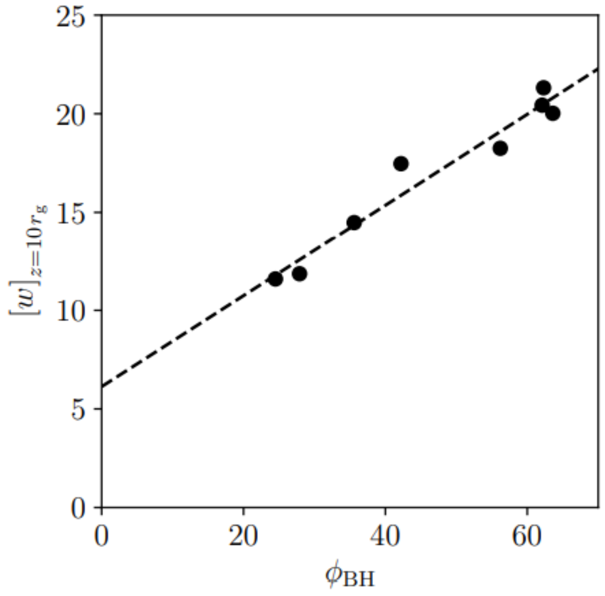

BH magnetic flux

R. Narayan, A. Chael, K. Chatterjee, A. Ricarte, B. Curd
arXiv: 2108.12380

Jet Power & Width in long-duration MAD Simulations

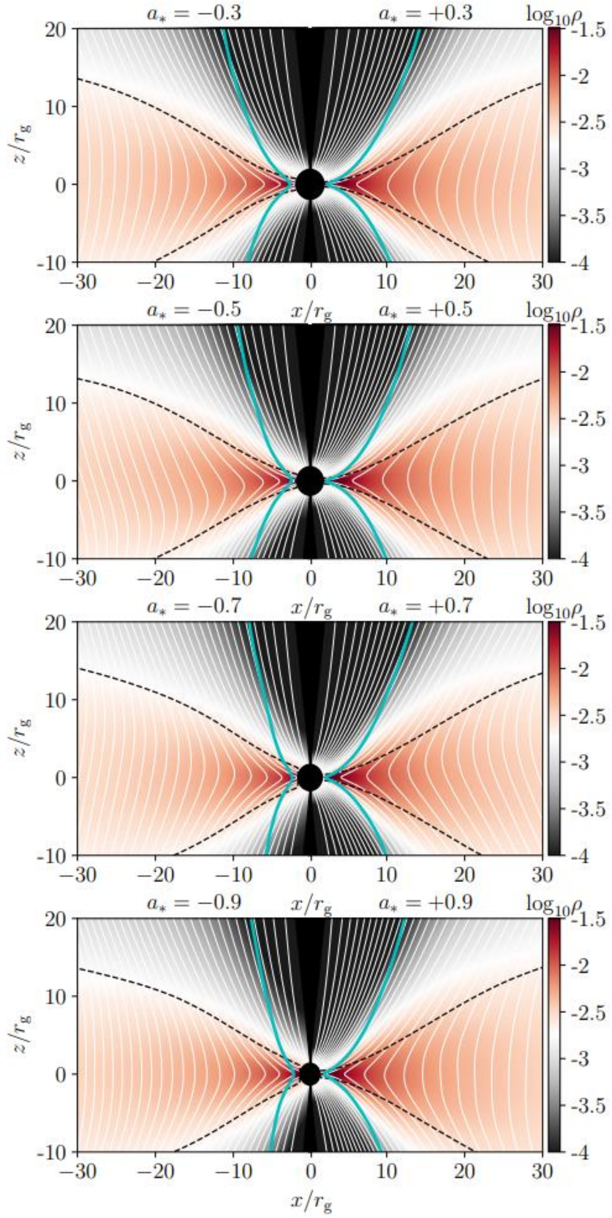

Time-and azimuth-averaged simulation data

- Magnetic flux on the BH in MAD simulations saturates at different values depending on the BH spin
- Retrograde disks saturate at lower magnetic flux values

Magnetic flux though the horizon

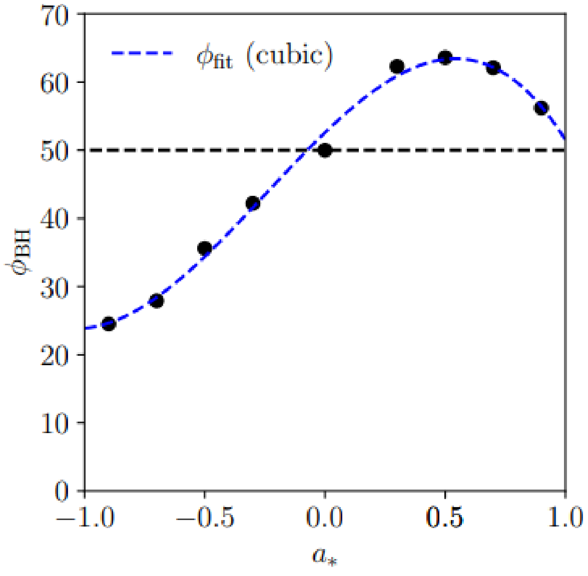

Jet efficiency

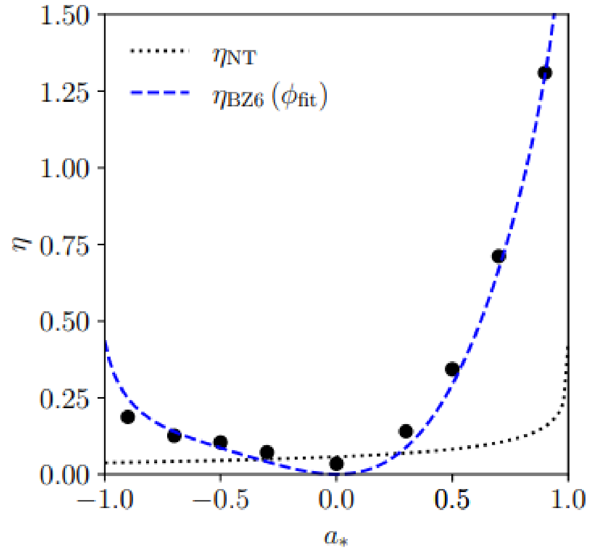

BH spin

R. Narayan, A. Chael, K. Chatterjee, A. Ricarte, B. Curd
arXiv: 2108.12380

Another high-dynamic range feature

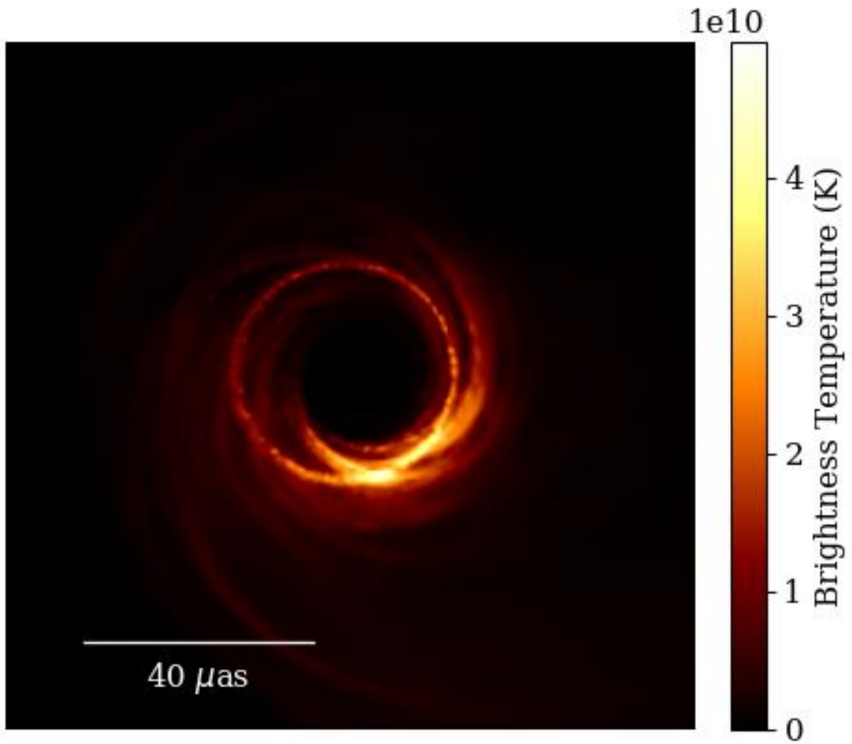

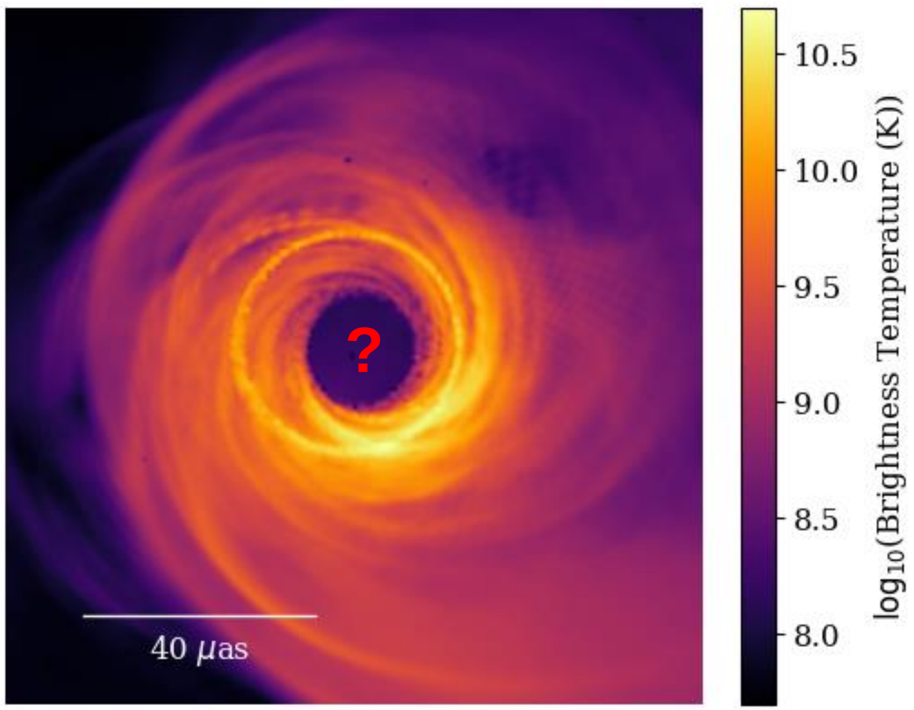

This sharp brightness depression in high-dynamic range simulation images corresponds to what we call the **BH "inner shadow" –** closely tracing the lensed image of the event horizon in the equatorial plane

A. Chael, M. Johnson, A. Lupsasca
arXiv: 2106.00683

The Critical Curve & “Black Hole Shadow”

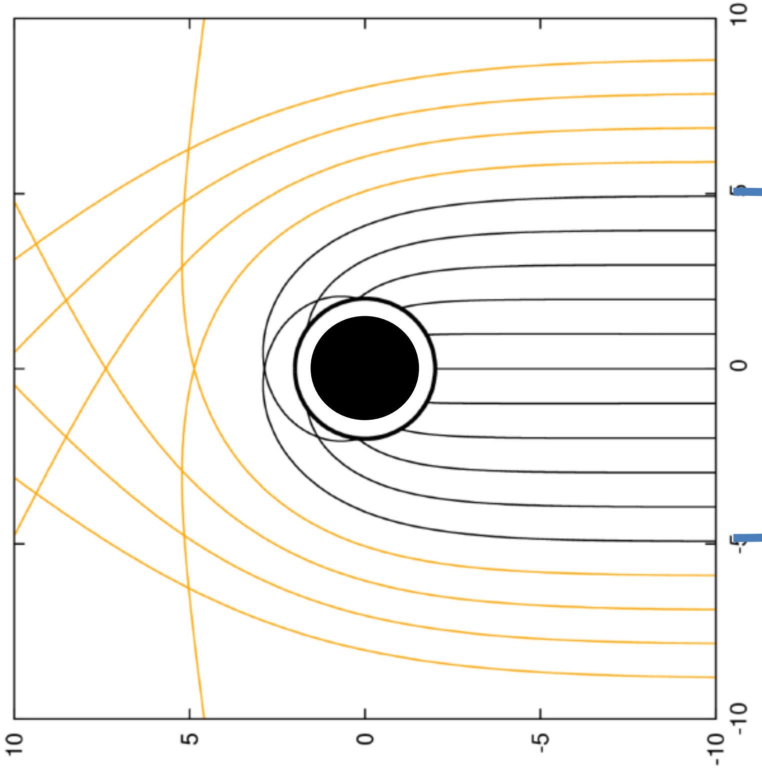

$$d_{\mathrm{shadow}} = 2\sqrt{27}GM/c^2$$

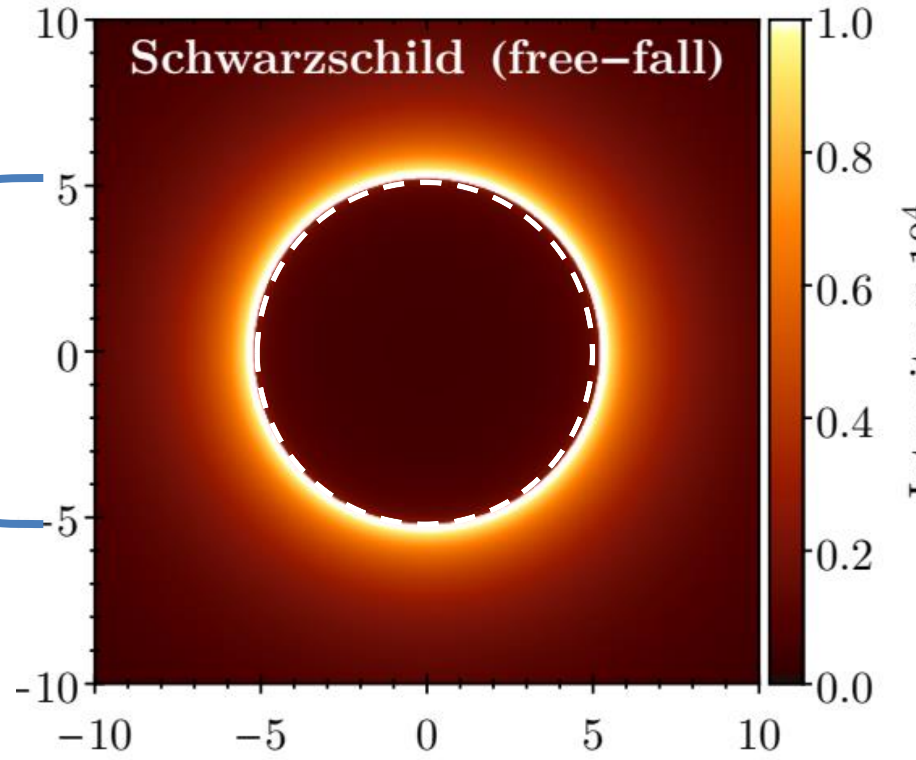

- The ‘critical curve’ on the image separates of rays that end on the event horizon with those that escape to infinity
- The interior of the critical curve is the ‘black hole shadow’, where all rays end on the horizon
- The shadow is particularly prominent as an image feature when the emission is optically thin and **spherically symmetric**

Image credit: Keiichi Asada
Narayan+ 2019 (also Falcke+ 2000, many others)

Lensed images of the **equatorial plane**

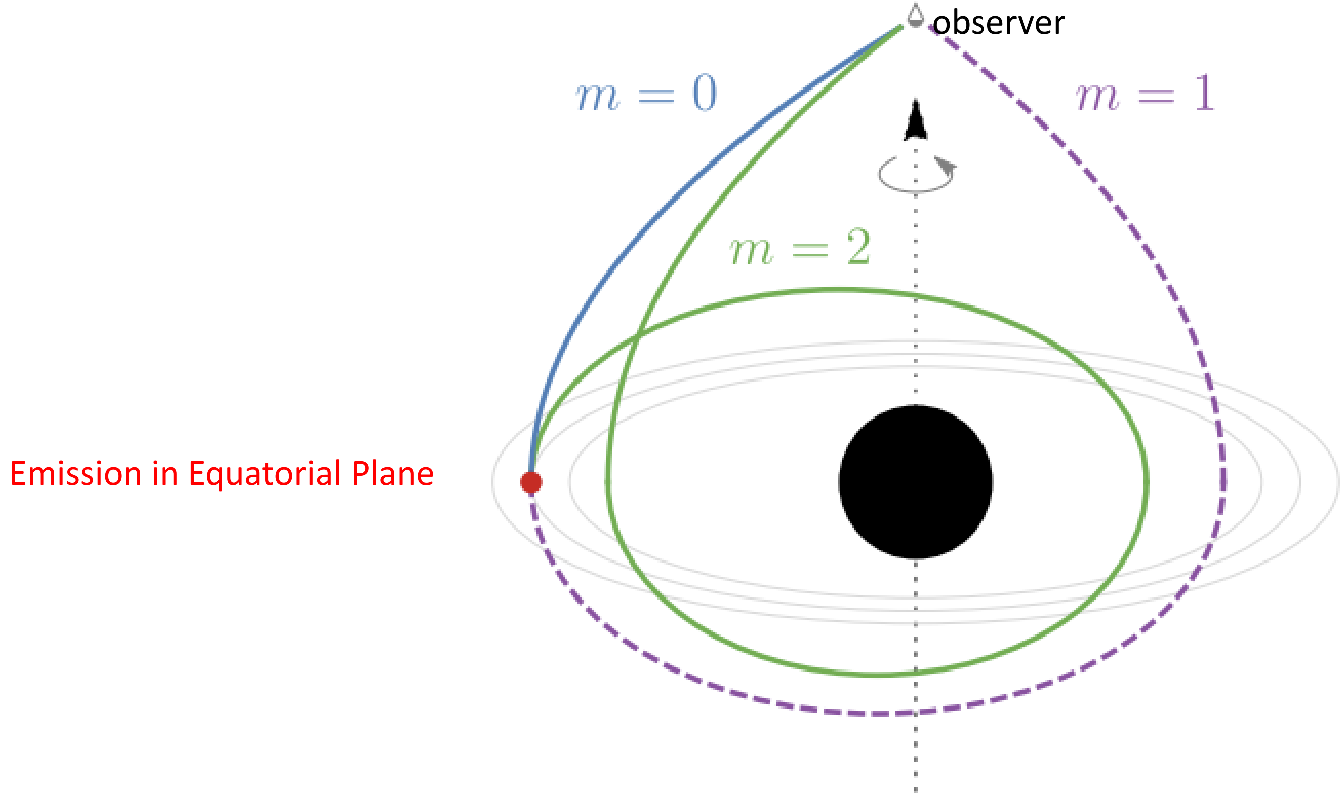

Image credit: Gralla & Lupsasca 2019

Photon Rings

Time-averaged GRMHD

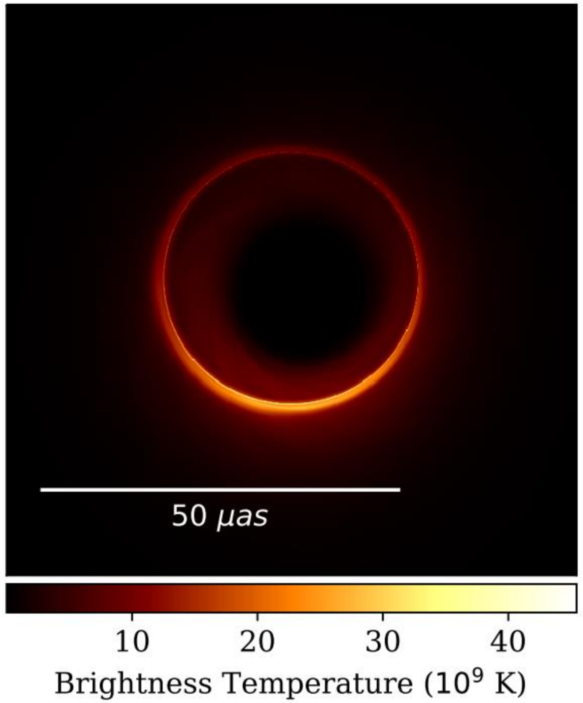

Angular slices (image)

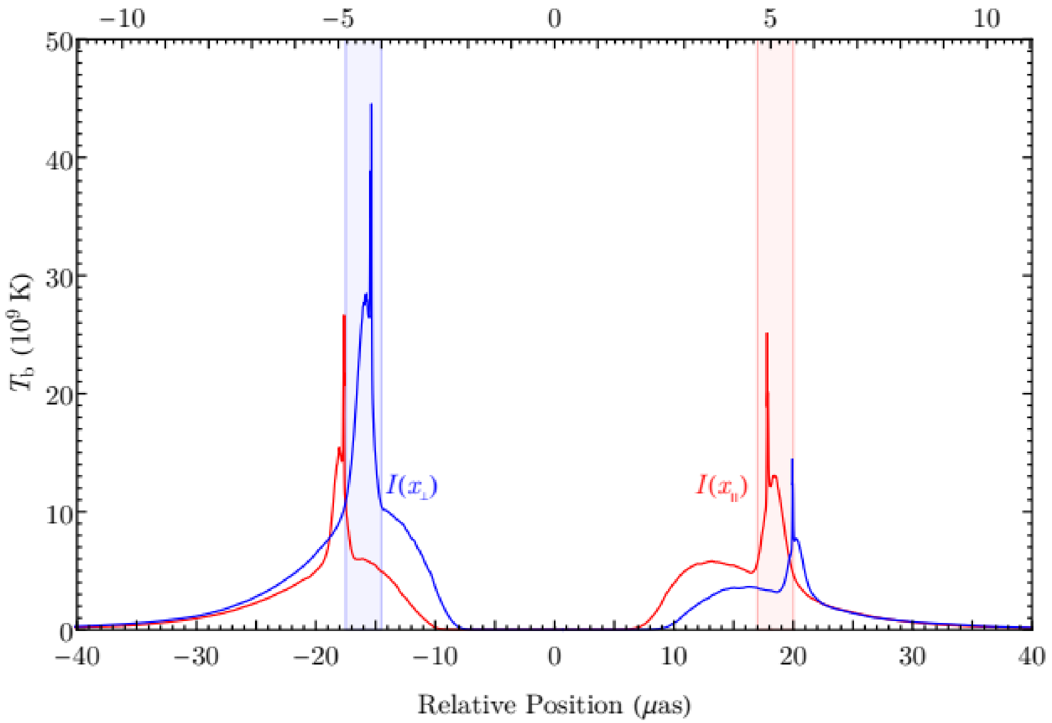

- As geodesics wrap around the black hole multiple times, they form a **series of images** lensed into **increasingly narrow rings**
- These subrings approach the critical curve exponentially.
- Distinguishing the subrings requires a **spatially limited emission region** (e.g. emission confined to the equatorial plane)

Johnson+ 2019
Arxiv: 1907.04329

Photon Rings

Time-averaged GRMHD

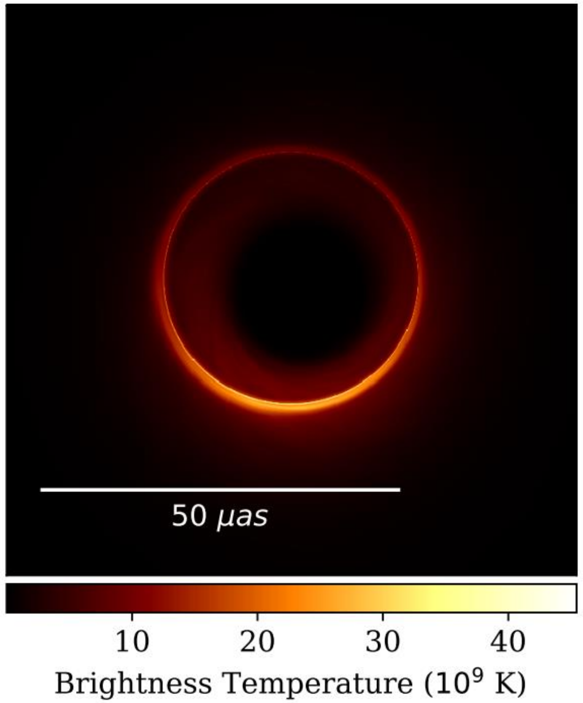

Angular slices (visibility)

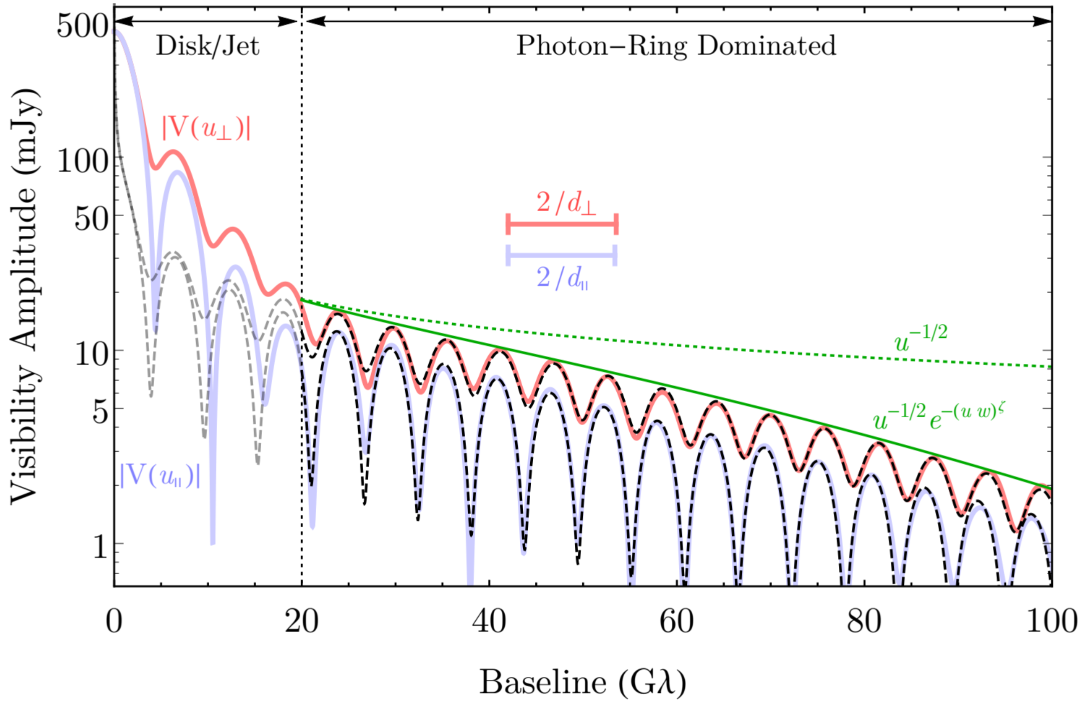

- As geodesics wrap around the black hole multiple times, they form a **series of images** lensed into **increasingly narrow rings**
- These subrings approach the critical curve exponentially.
- Distinguishing the subrings requires a **spatially limited emission region** (e.g. emission confined to the equatorial plane)
- A VLBI experiment with extremely long baselines (e.g. to space) could directly detect & measure the photon ring(s)

Johnson+ 2019
Arxiv: 1907.04329

Lensed images of the equatorial plane

Curve: n=0 image of the equatorial event horizon

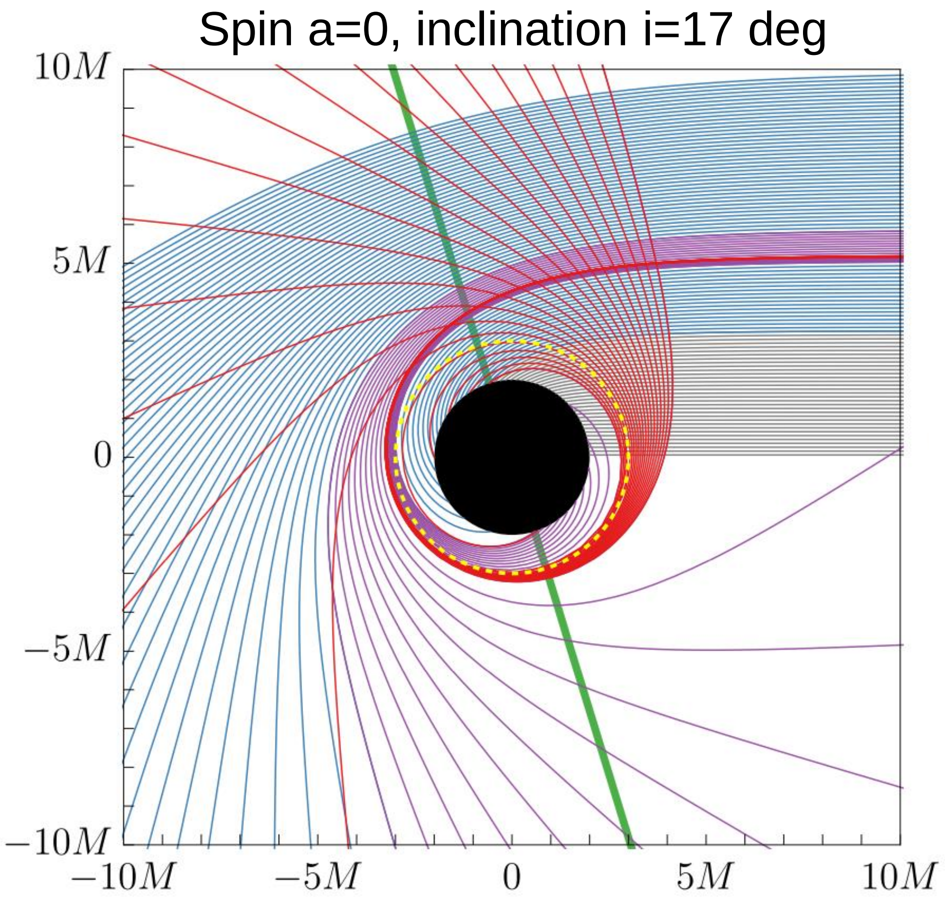

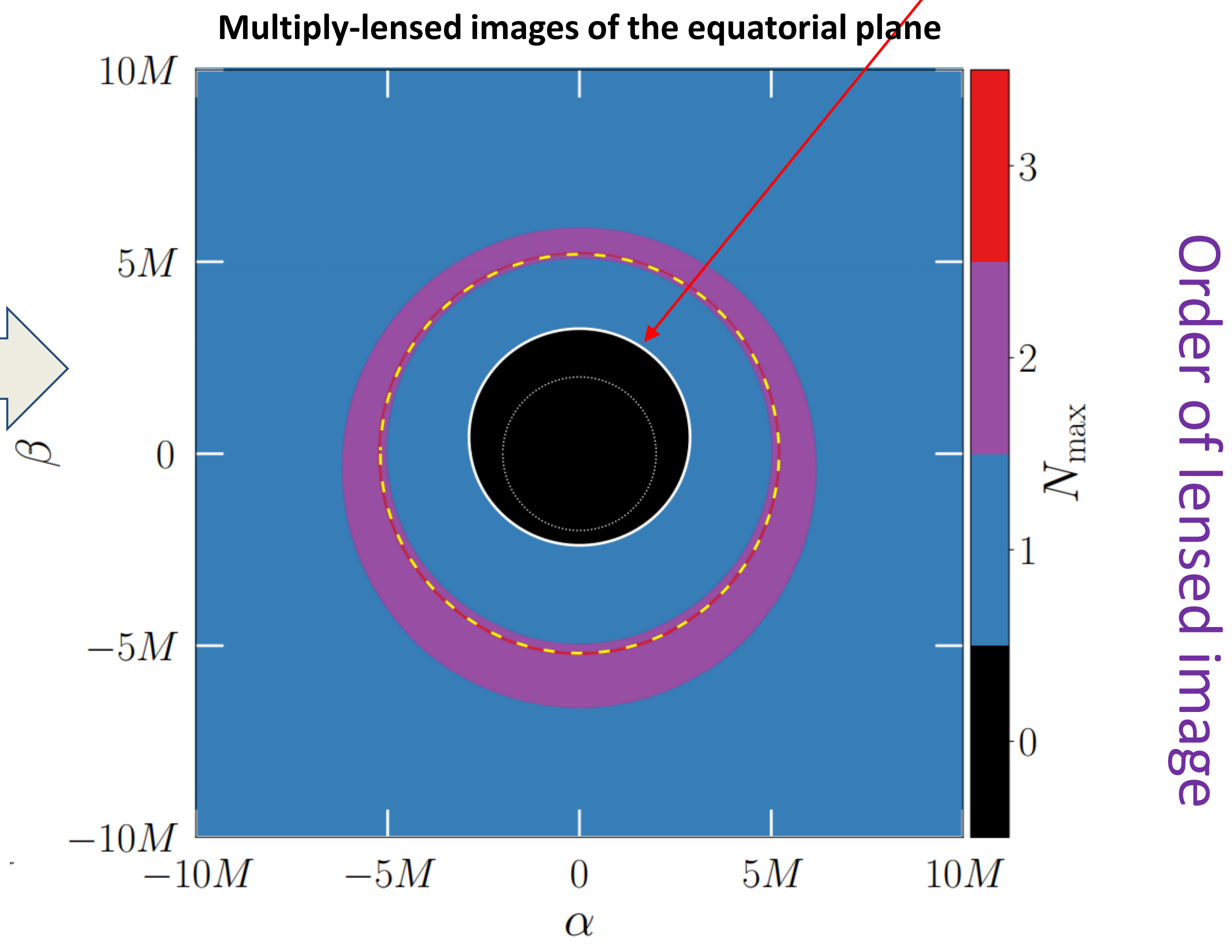

This feature has been discussed many times in analytic models in e.g.:

- Luminet 1979, Figure 2
- Takahashi 2004, Figure 1
- Gralla, Holz, Ward 2019, Figure 1
- Dokuchaev 2019

A. Chael, M. Johnson, A. Lupsasca
arXiv: 2106.00683

Inner shadow in GRMHD images

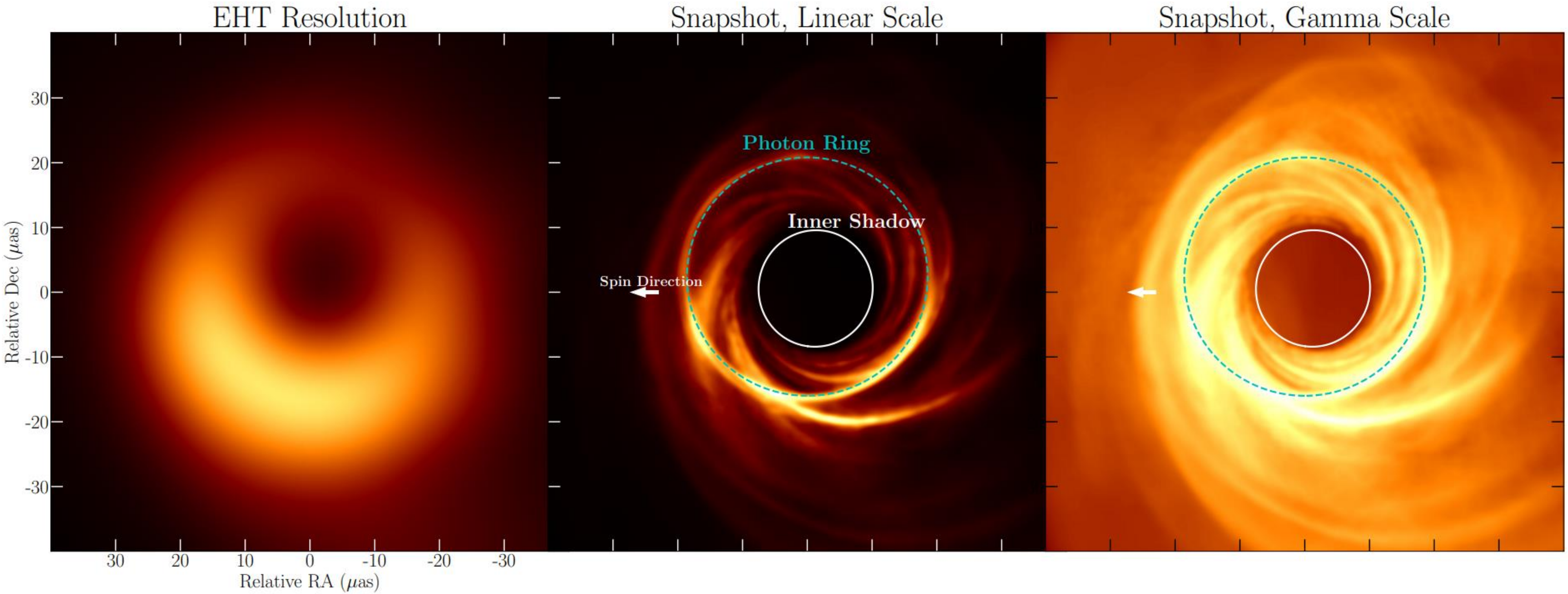

- This high dynamic range feature approaches the **lensed image of the equatorial event horizon**

Why is the inner shadow visible in these simulations?

Emissivity proxy (same as in Porth+ 2019)

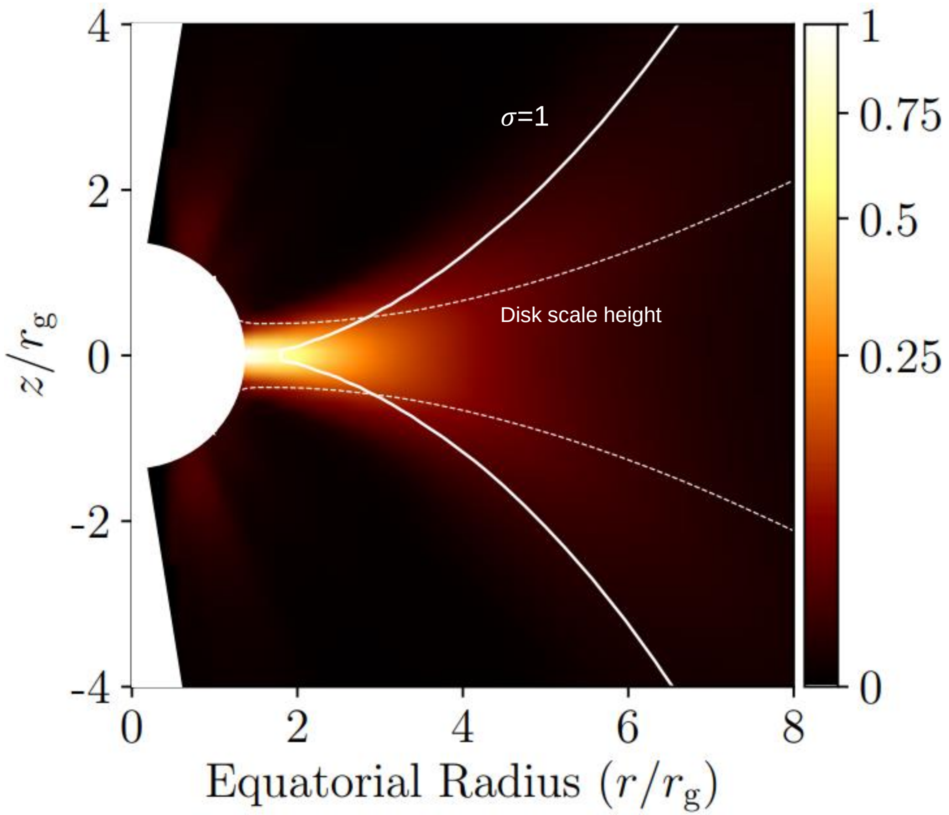

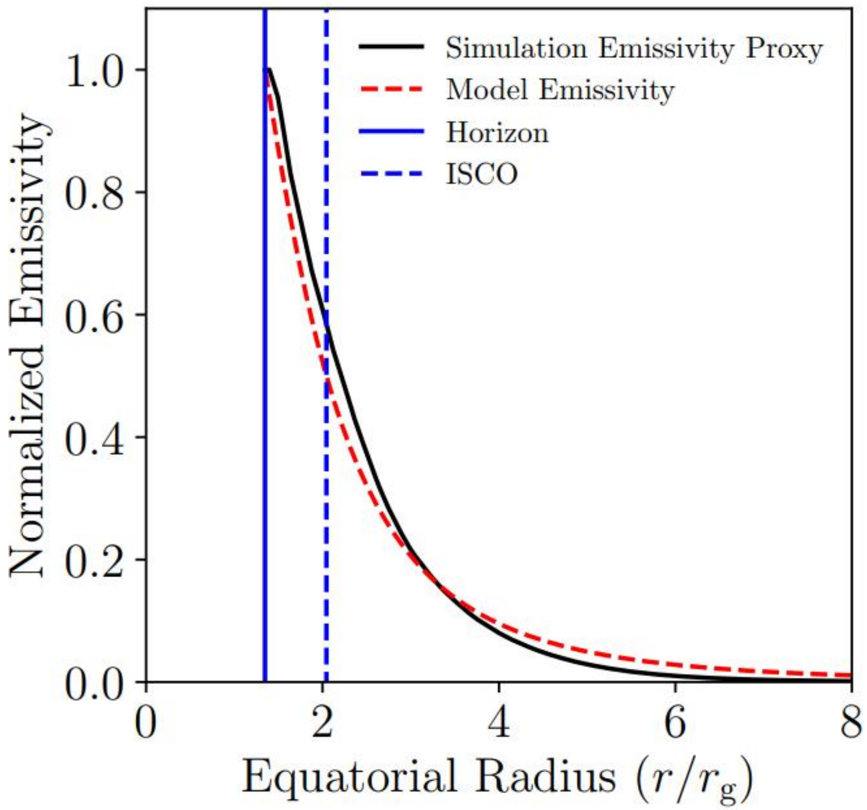

Equatorial slice

- The 230 GHz emissivity is predominantly **equatorial** in this simulation
- It does not truncate at the ISCO, but **extends to the horizon**
- Fluid velocities are **subkeplerian** – reducing the overall redshift

Time-averaged simulation images at high dynamic range

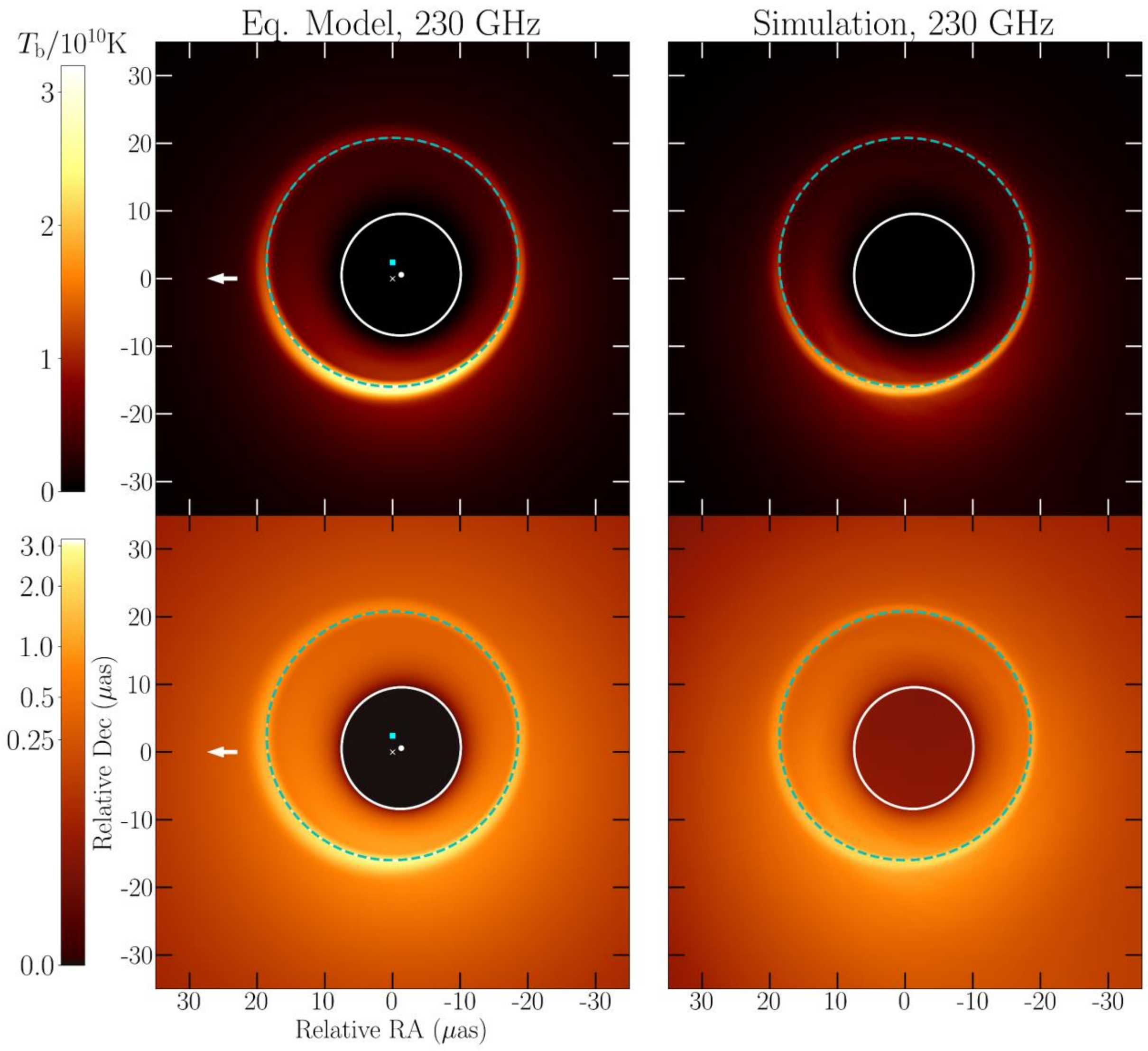

- The averaged simulation image shares the **primary features of an image from a purely equatorial disk model** (Gralla,Lupsasca,Marrone+ 2020)
- **Forward jet emission** in the simulation gives the horizon image a finite “floor”

230 GHz emission profiles

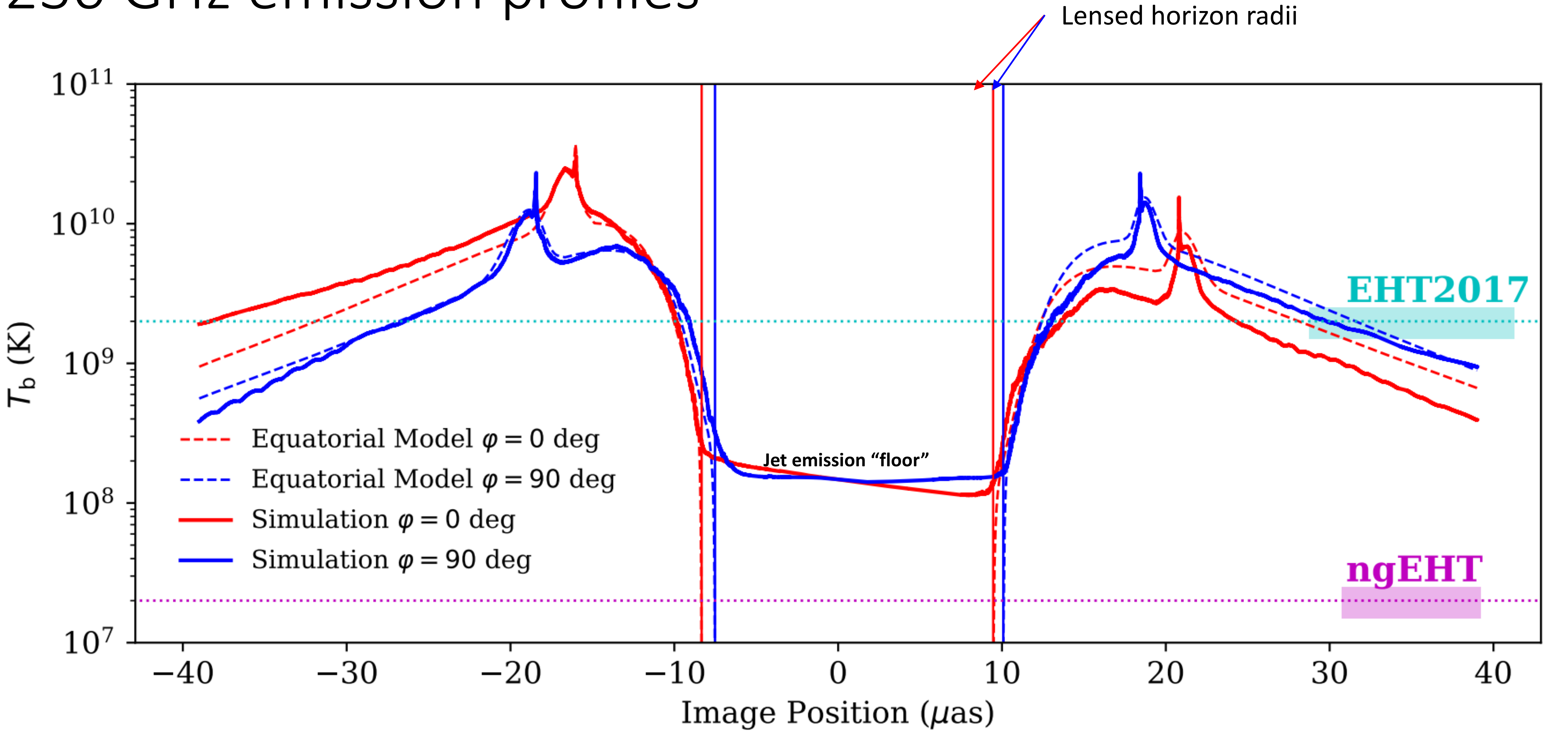

The ngEHT should have the dynamic range to observe the inner shadow feature, if present

EHT 2017 and ngEHT image reconstructions

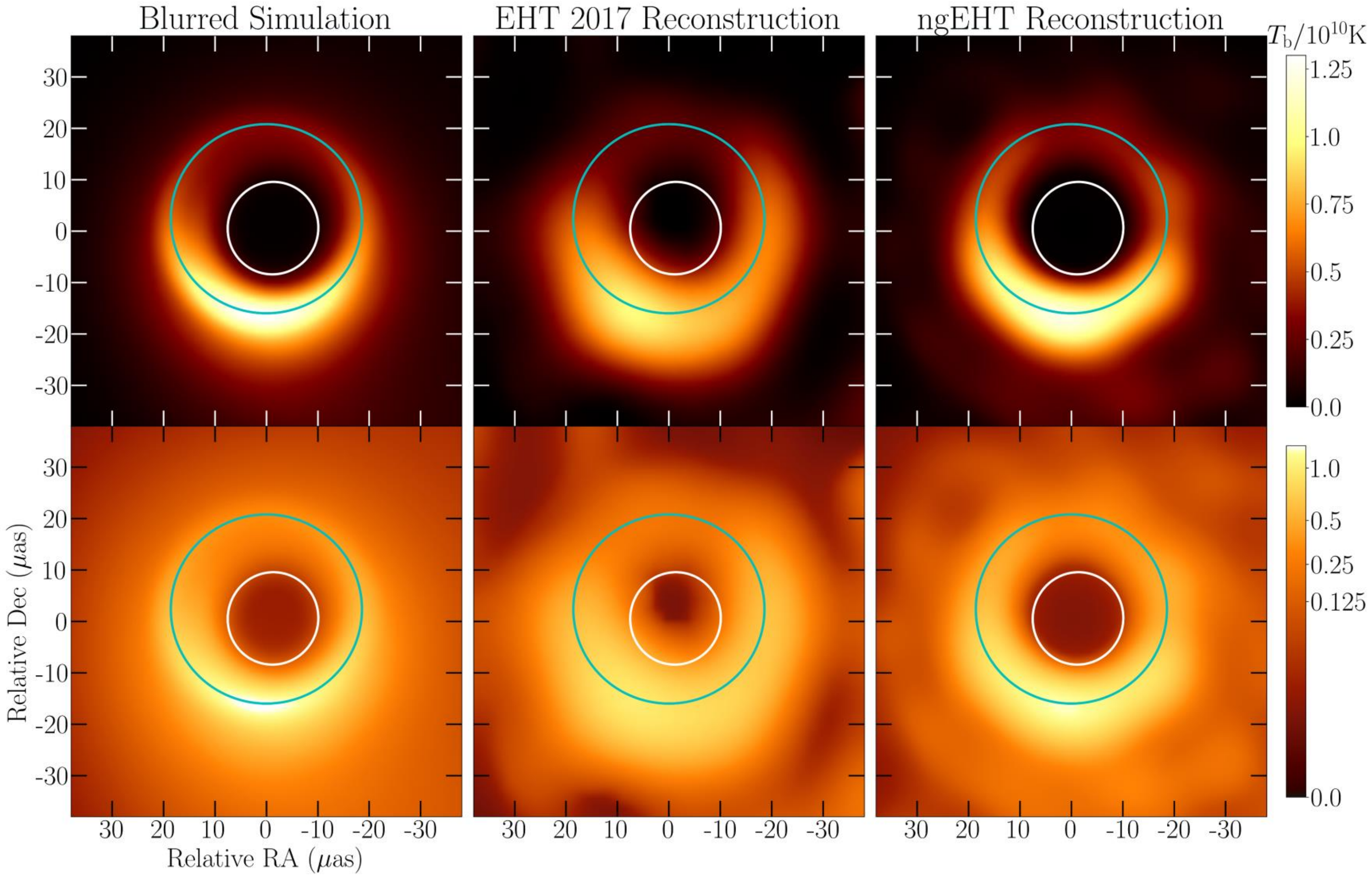

- ‘Realistic’ EHT imaging scripts using closure phases and amplitudes, but on the time-averaged image
- **Imaging algorithms can detect the inner shadow in ngEHT data** – analytic modeling may constrain its shape more precisely

Inner shadow images provide another probe of spacetime

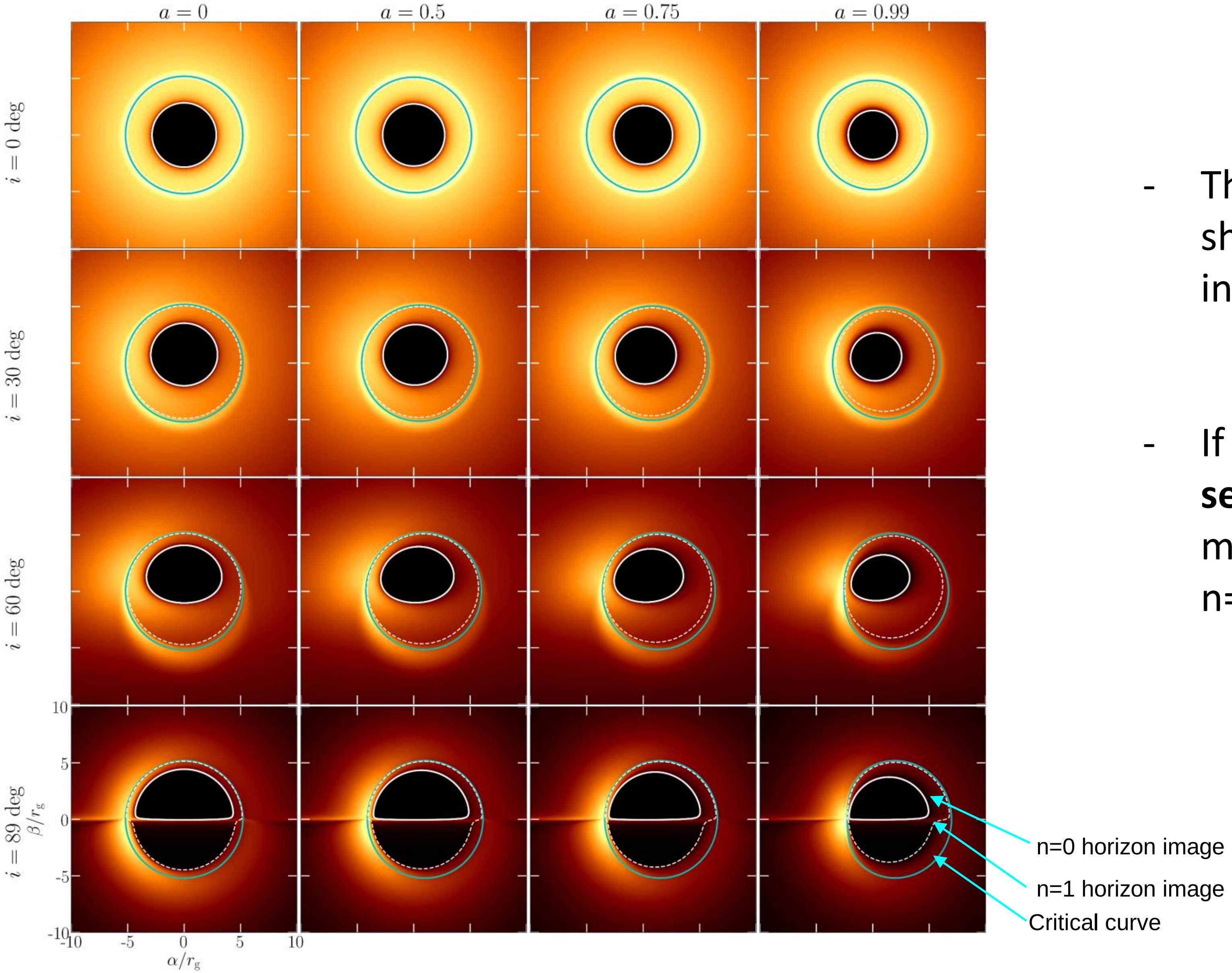

- The horizon image changes in shape and size with spin and inclination

- If observable, it would provide a **second set of constraints** on the metric from observations of the n=1 photon ring

Properties of the lensed horizon image

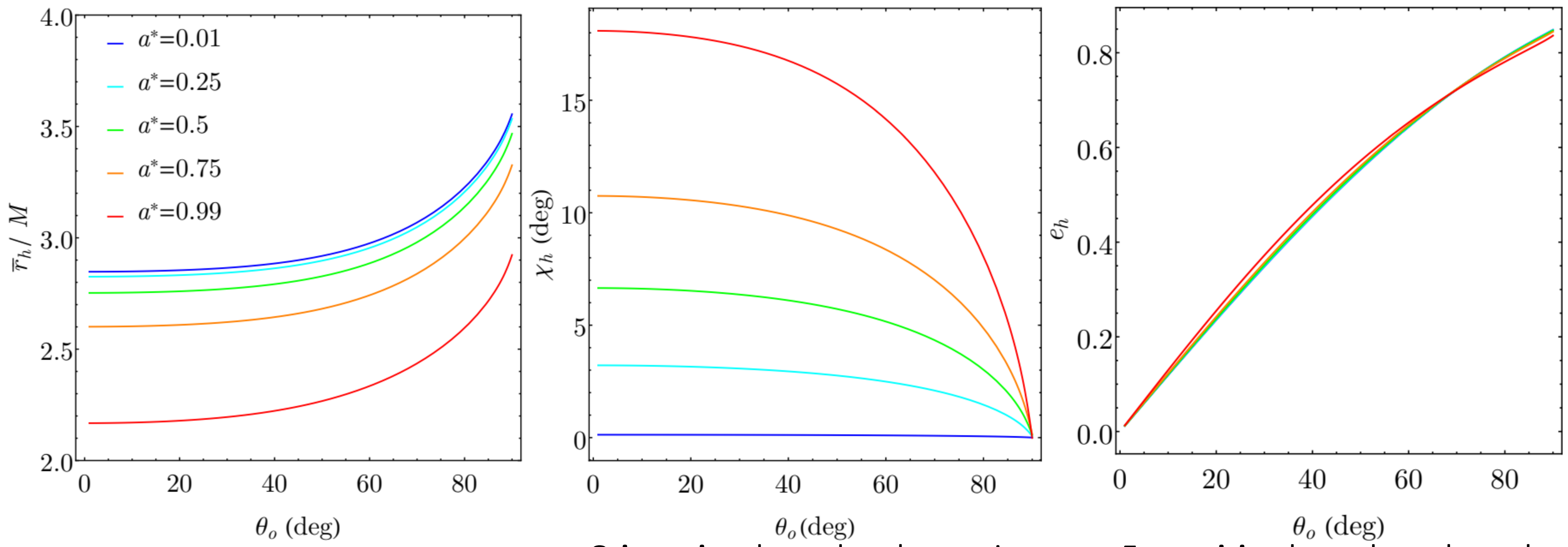

Radius depends mostly on spin at low inclination

Orientation depends only on spin at low inclinations

Eccentricity depends ~only on the inclination at all spins

The face-on inner shadow size changes by **~40% from spin 0 to spin 1**, while the shadow/photon ring size changes by only 4% (Johannsen+Psaltis 2010)

Relative centroid and relative radius

With **two** curves in the image (horizon and photon ring/shadow),
we can measure **relative** offsets and sizes and remove the effect of uncertain mass

Horizon/Critical Curve radius ratio

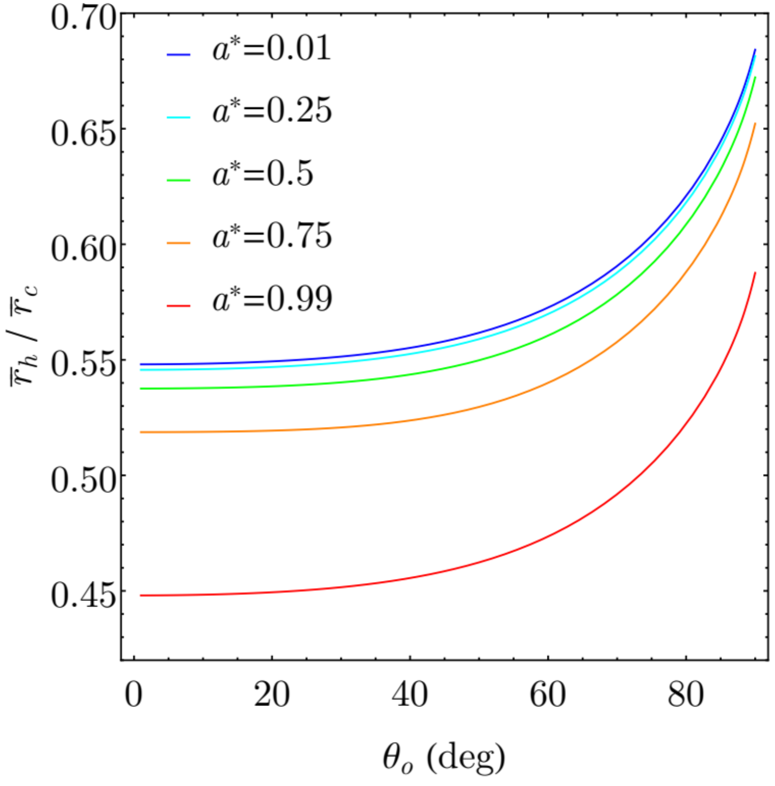

At low inclination, horizon-to-shadow size
Is **spin-dependent** and decreases from
55% to 45% from a=0 to a=1

Horizon-Critical Curve centroid offset

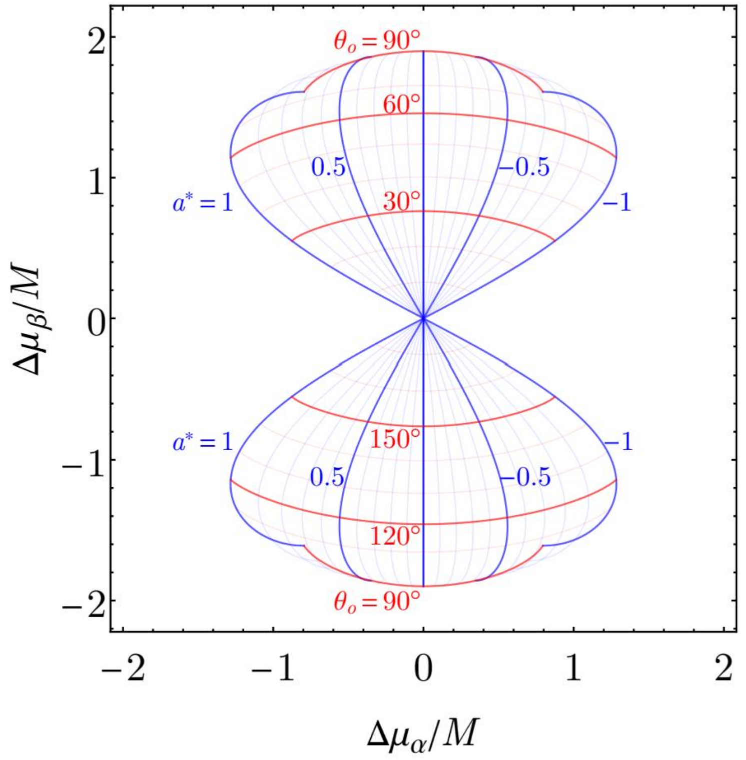

Centroid offset:
angle depends on spin,
magnitude on inclination

$$a \approx -1.64 \arctan\left(\pm_o 0.61 \Delta\alpha / \Delta\beta\right)$$

$$\theta_o \approx \pm_{\Delta\beta} 0.42 \sqrt{\Delta\alpha^2 + (\Delta\beta/0.61)^2}.$$

Relative centroid and relative radius: toy example

Measurements of both the inner shadow and photon ring at fixed M87* inclination
Error bands for uncertainties of 0.1, 0.5, 1 uas

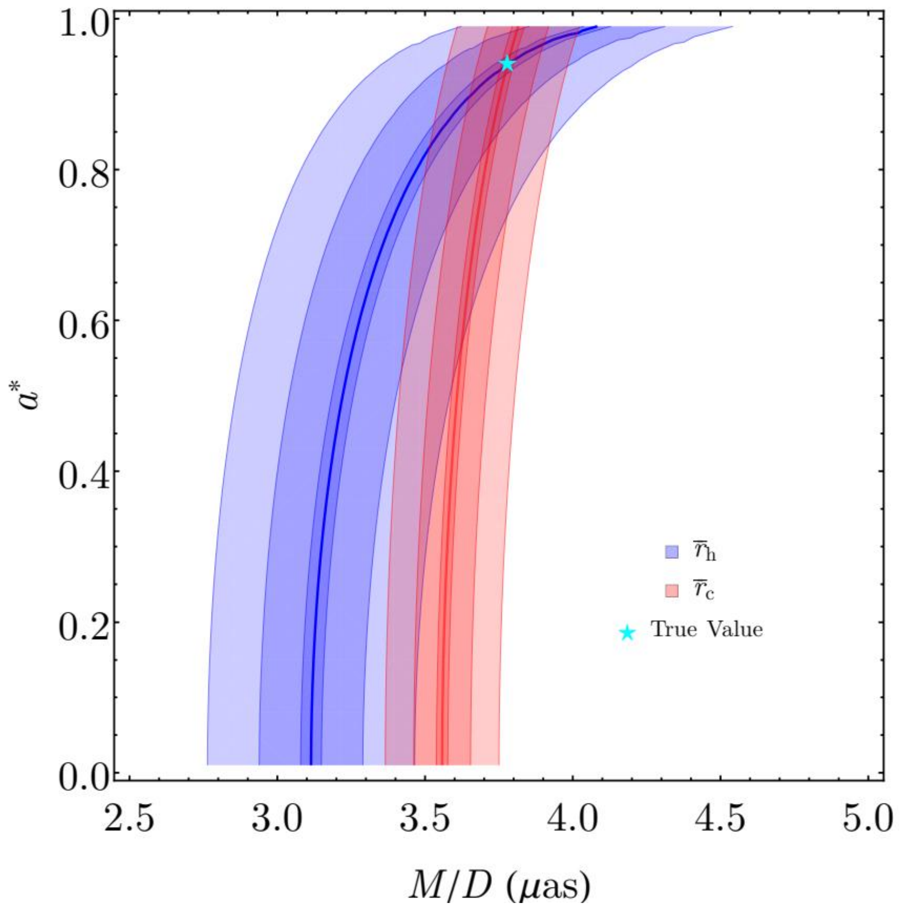

Inner shadow & photon ring sizes

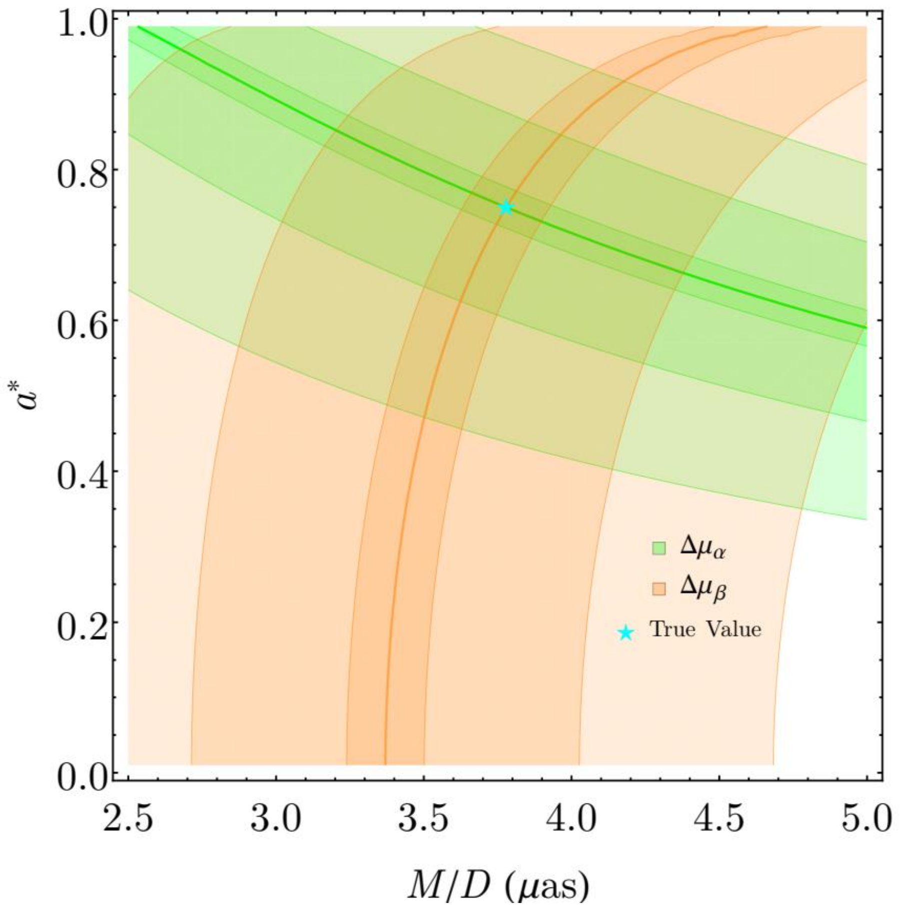

Centroid offset

What might we see in M87* with future observations or a next-generation EHT array?

A: According to current simulations, a wide, horizon-scale jet base and an “inner shadow” close to the position of the lensed event horizon

Outline

1. Q: What do polarized images of M87* tell us about the magnetic fields near the supermassive black hole?

A: Magnetic fields in M87* are strong and dynamically important: the accretion flow is **magnetically arrested**

2. Q: What might we see in M87* with a next-generation EHT array?

A: According to current simulations, a wide, horizon-scale jet base and an “inner shadow” close to the position of the lensed event horizon

Thank you!